The Plant Cell, Vol. 18, 3686–3705, December 2006, www.plantcell.org © 2006 American Society of Plant Biologists

A Multidrug Resistance Transporter in *Magnaporthe* Is Required for Host Penetration and for Survival during Oxidative Stress [W]

Chuan Bao Sun, Angayarkanni Suresh, Yi Zhen Deng, and Naweed I. Naqvi[1]

Fungal Patho-Biology Group, Temasek Life Sciences Laboratory and Department of Biological Sciences, National University of Singapore, Singapore 117604

In prokaryotes and eukaryotes, multidrug resistance (MDR) transporters use energy-dependent efflux action to regulate the intracellular levels of antibiotic or xenobiotic compounds. Using mutational analysis of *ABC3*, we define an important role for such MDR-based efflux during the host penetration step of *Magnaporthe grisea* pathogenesis. Mutants lacking *ABC3* were completely nonpathogenic but were surprisingly capable of penetrating thin cellophane membranes to some extent. The inability of *abc3Δ* to penetrate the host surface was most likely a consequence of excessive buildup of peroxide and accumulation of an inhibitory metabolite(s) within the mutant appressoria. Treatment with antioxidants partially suppressed the host penetration defects in the *abc3Δ* mutant. *abc3Δ* was highly sensitive to oxidative stress and was unable to survive the host environment and invasive growth conditions. *ABC3* transcript levels were redox-regulated, and on host surfaces, the activation of *ABC3* occurred during initial stages of blast disease establishment. An Abc3-green fluorescent protein fusion localized to the plasma membrane in early appressoria (and in penetration hyphae) but became predominantly vacuolar during appressorial maturity. We propose that *ABC3* function helps *Magnaporthe* to cope with cytotoxicity and oxidative stress within the appressoria during early stages of infection-related morphogenesis and likely imparts defense against certain antagonistic and xenobiotic conditions encountered during pathogenic development.

INTRODUCTION

Transmembrane proteins belonging to the ubiquitous ATP binding cassette (ABC) superfamily have been identified in several genera representing prokaryotes and eukaryotes (Higgins, 1992). Identification and subsequent sequence comparisons of >100 genes encoding ABC transporters revealed that the ABC proteins possess one or two well-conserved nucleotide binding folds of ~200 amino acid residues and contain the Walker A and B motifs and the SGG(Q) signature (Michaelis and Berkower, 1995). Several members of this large superfamily function in the transport of cytotoxic agents across biological membranes and help maintain a reduced intracellular level of toxins or metabolites (Driessen et al., 2000). ABC transporters play a major role in the multidrug resistance (MDR) mechanism that operates in mammalian tumor cells. The MDR subfamily of efflux pumps includes the MDR P-glycoproteins. Several MDR-type P-glycoproteins have been shown to catalyze the ATP-dependent efflux of antitumor agents during chemotherapy of cancer cells (Cole et al., 1992; Gottesman and Pastan, 1993). In addition, a number of P-glycoproteins of the MDR family have been implicated in the active extrusion or maintenance of a broad range of compounds, namely, solutes, peptides, hormones, lipids, and drugs (Kolaczkowski et al., 1998).

The ascomycete *Magnaporthe grisea* causes blast disease in several monocot plant species (Ou, 1985), including rice (*Oryza sativa*), and represents a model system to study fungal plant interaction (Valent, 1990). To breach the plant surface, the asexual spores or conidia of *Magnaporthe* elaborate a specialized infection structure termed appressorium. Upon entry into the host cells, the fungus proliferates by forming penetration hyphae and infection hyphae that help in establishing and spreading the disease (reviewed in Hamer and Talbot, 1998; Talbot, 2003).

Phytopathogenic fungi need to adapt to their specific host environment and subsequently overcome the cytotoxic and antifungal compounds or phytoalexins produced by the plant hosts (Kodama et al., 1992; Dixon et al., 1994; Osbourn, 1996). In filamentous fungi, ABC transporter activity likely involved in energy-dependent efflux of fungicides or phytoalexins has been reported in *Aspergillus nidulans* (Andrade et al., 2000), *Aspergillus fumigatus* (Tobin et al., 1997), *Botrytis cinerea* (Vermeulen et al., 2001), *Magnaporthe* (Urban et al., 1999), *Gibberella pulicaris* (Fleissner et al., 2002), and *Mycosphaerella graminicola* (Stergiopoulos et al., 2003; Zwiers et al., 2003). However, none of these molecules belong to the P-glycoprotein MDR subfamily of the ABC transporters.

In this study, we report the identification and characterization of a novel insertional mutant in *Magnaporthe* that showed a complete loss of pathogenicity toward host plants. The disrupted gene locus, termed *ABC3*, encodes an MDR protein with extensive homology to the Cluster II.2–type P-glycoprotein transporters,

[1] To whom correspondence should be addressed. E-mail naweed@tll.org.sg; fax 65-6872-7007.
The author responsible for distribution of materials integral to the findings presented in this article in accordance with the policy described in the Instructions for Authors (www.plantcell.org) is: Naweed I. Naqvi (naweed@tll.org.sg).
[W] Online version contains Web-only data.
www.plantcell.org/cgi/doi/10.1105/tpc.105.037861

such as MDR1 in humans. We show that loss of Abc3 protein leads to cessation of the infection-related morphogenesis at the host penetration step. Consequently, mutants lacking *ABC3* were incapable of breaching host surfaces, and although inefficiently, were still able to penetrate artificial substrates like cellophane. We show that *ABC3* itself is regulated in a redox-responsive manner and likely by a plant signal(s). An interesting finding relates to the involvement of *ABC3* in regulating the fungal response to oxidative stress, suggesting that Abc3 protein serves as a novel MDR that is necessary for pathogenicity and the ability of the blast fungus to withstand oxidative damage and the host-specific adverse environment.

RESULTS

Identification and Isolation of the *ABC3* Locus

In an *Agrobacterium tumefaciens* T-DNA–based forward genetics approach in *Magnaporthe*, a mutant strain TMT2807 was identified due to its dramatic and total failure to infect the barley (*Hordeum vulgare*) cultivar Express (Figure 1A). Further monoconidial and random ascospore analysis–assisted purification of TMT2807 showed that the pathogenesis defect cosegregated with hygromycin resistance, conferred by a single copy integration of the *HPH1*-containing T-DNA in this strain (Figures 1B and 1C; see Materials for details). Thermal asymmetric interlaced PCR analysis (Liu et al., 1995) revealed that the T-DNA insertion in TMT2807 disrupted the genomic region corresponding to Contig 67 on Supercontig 5.117 (*Magnaporthe* Genome Database, Release 5, Broad Institute). Further subcloning and sequence analysis showed that the T-DNA insertion in TMT2807 disrupted a region just proximal (231 bp upstream) to exon 1 of open reading frame (ORF) MGG_13762.5 (Figure 1B) and led to a total loss of transcription of this ORF (data not shown). Analysis of the BAC clone 22C21 (identified using the T-DNA insertion flanks from TMT2807 as probes) revealed the presence of the ORF mentioned above as a 6.3-kb *Hin*dIII fragment (Figure 1B). We designated this gene as *ABC3* because its predicted product showed a high degree of sequence similarity to the ABCs encoded by the genes belonging to the ABC transporter superfamily.

Characteristics of the *ABC3* Gene and Protein

The *ABC3* locus spanned nucleotides 124832 to 131097 on Supercontig 177 (Figure 1B). We obtained a full-length *ABC3* cDNA by 3′ and 5′ rapid amplification of the cDNA ends (RACE) and by several RT-PCR fragments representing the overall *ABC3* coding sequence. In each instance, DNA sequence analysis was performed on both the strands of at least two independent clones. Subsequent analysis revealed the existence of 13 exons (Figure 1B) in the *ABC3* ORF as opposed to the autocall-predicted 11 exons in MGG_13762.5. In addition, three nucleotide changes were uncovered in exon 3 of MGG_13762.5. The complete nucleotide sequence and annotation details for *ABC3* have been deposited in GenBank under accession number DQ156556. Typical regulatory elements related to fungal promoter regions preceded the *ABC3* ORF. Based on the cDNA sequence, the *ABC3* gene was predicted to encode a 1321–amino acid protein (hereafter, Abc3p) composed of two homologous halves, each with six membrane-spanning segments (ABC transmembrane domain) and an ABC ATPase motif. Abc3p thus showed an overall structure and domain organization typical of the Cluster II.2–type (or Transport Commission number

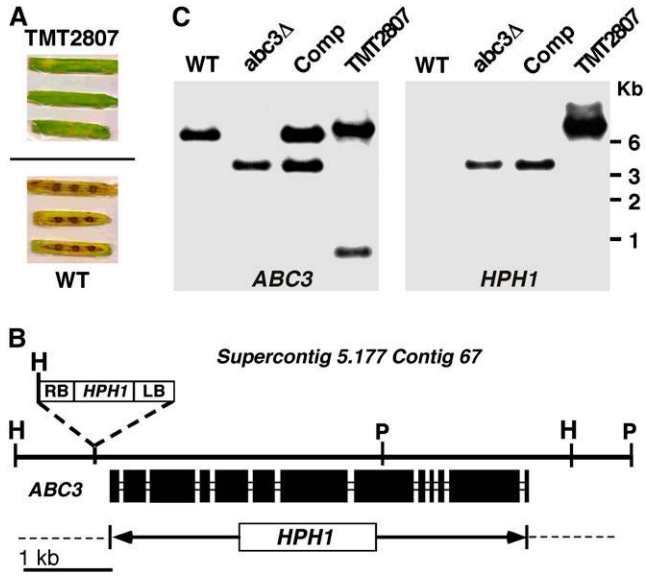

Figure 1. Identification and Characterization of the TMT2807 Mutant.

(A) Barley leaf explants were inoculated with conidiospores of TMT2807 strain or wild-type *Magnaporthe* and disease symptoms assessed after 9 d.

(B) Schematic representation of the annotated *ABC3* locus spanning a *Hin*dIII-*Pvu*II fragment from Contig 67 on Supercontig 5.117 in *Magnaporthe*. Closed bars and short open boxes indicate the coding regions and introns, respectively, and are drawn to scale. RB and LB represent the right and left border sequences of T-DNA (open box) integrated in the mutant strain. Opposing arrows demarcate the genomic region deleted in the *abc3Δ* strain that was created using flanking homology (dashed lines) based gene replacement with the hygromycin resistance cassette (*HPH1*). Restriction enzyme sites *Hin*dIII (H) and *Pvu*II (P) have been depicted. Bar = 1 kb and also denotes the probe used for DNA gel blot analysis shown in the next panel.

(C) DNA gel blot analysis of the *ABC3* mutants and the complemented strain. Genomic DNA from the wild type, *abc3Δ*, complemented strain (Comp; *abc3Δ* carrying an ectopic single-copy integration of the *Hin*dIII fragment described in **[B]** above), and TMT2807 strain was digested with *Hin*dIII and probed with the 1-kb *ABC3* fragment or the *HPH1*-specific fragment. The appearance of the 3.2-kb band in the *abc3Δ* strain, with the concomitant loss of the wild-type 6.3-kb *ABC3* locus, was diagnostic of the correct gene replacement event. Ectopic integration of the rescue construct in the complemented strain resulted in the retention of the 3.2-kb fragment and the restoration of the 6.3-kb band. The presence of a 0.6-kb fragment in the TMT2807 strain is due to an internal *Hin*dIII site at the right-border end of the integrated T-DNA in TMT2807. This integron also accounts for the ~7-kb fragment (the *ABC3* gene disrupted with *HPH1* T-DNA cassette) detected in this mutant. DNA gel blot analysis with *HPH1* as probe further confirmed the identity of the fragments described earlier. Molecular size markers in kilobase pairs are indicated.

3.A.1.201) P-glycoprotein MDR transporters (Decottignies and Goffeau, 1997; Saier and Paulsen, 2001).

Comparison of the Abc3 protein sequence with related sequences in SWISS-PROT and other protein sequence resources identified several members of the P-glycoprotein family of ABC transporters. A phylogenetic relationship was established using these sequences (Figure 2). Individual sequence comparisons and phylogenetic analyses based on ClustalW (Thompson et al., 1994; see Supplemental Figure 1 online), MEGA (Kumar et al., 2004), and Phylip 3.6a (Felsenstein, 1989) revealed that Abc3p likely defines a separate family of fungal MDR transporters distinct from the Pmd1 or the ATRC family (Figure 2, arrows). The phylogram also showed that Abc3p had diverged significantly from its most related Ste6 protein in *Saccharomyces cerevisiae* (Figure 2). However, there was a paralogous transporter (MG09931.4; 56% similarity) encoded in *Magnaporthe* (Figure 2). Rather surprisingly, neither Abc3p nor MG09931.4 showed any significant similarity (average 7% similarity and 4% identity) to the Abc1 (Urban et al., 1999) or Abc2 transporter (Lee et al., 2005) reported in *Magnaporthe*. Abc3 showed the highest similarity to SNOG_05968 from *Phaeosphaeria* (62% similarity and 43% identity) and was found to be closely related to AtrC from *A. nidulans* (34% identity and 53% similarity), the fission yeast Pmd1 (54% similarity and 35% identity; Nishi et al., 1992), and the budding yeast Ste6 (46% similarity and 28% identity; Ketchum et al., 2001), whereas Abc1 showed a higher level of similarity to the ScPdr5 and CaCDR1 transporters from yeasts (see Supplemental Figures 2 and 3 online).

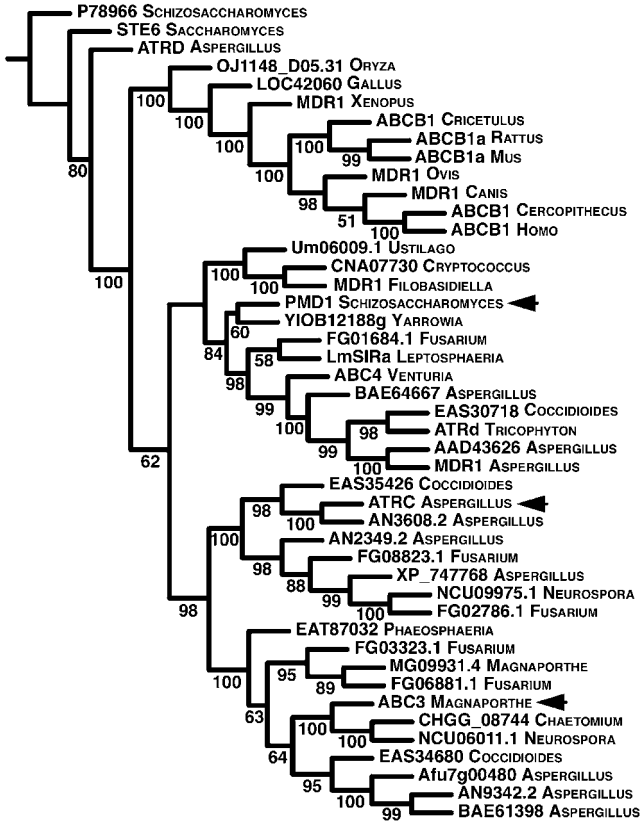

Figure 2. Phylogram of MDR Proteins Related to Abc3p.

ClustalW (Thompson et al., 1994) and Phylip 3.6a (Felsenstein, 1989) assisted dendrogram depicting the most parsimonious phylogenetic relatedness of *Magnaporthe* Abc3p with the MDR proteins from the indicated genera within eukaryotes. Bootstrapping (500 replicates/iterations) was used in generating the phylogenetic tree using the neighbor-joining algorithm in Phylip 3.6a. Percentage bootstrap support for each clade (when >50%) is indicated below the branch. B-Link web tool on the National Center for Biotechnology Information (NCBI) network was initially used to select 44 MDR hits related to Abc3p.

Phenotypic Characterization of the *abc3Δ* Strain

Using plasmid vector pFGLabcKO in a one-step gene replacement technique, we created an *ABC3* deletion mutant (hereafter referred to as *abc3Δ*) by replacing the entire 4.61-kb coding region of the *ABC3* locus (Figures 1B and 1C) with the *HPH1* cassette encoding the hygromycin phosphotransferase function. Hygromycin-resistant transformants (*HPH1*$^+$) derived from the wild-type Guy11 strain carrying single-copy insertion of the replacement cassette were identified, and the desired gene replacement event (*abc3*::*HPH1*) was confirmed by DNA gel blotting (Figure 1C, details in the figure legend). For complementation analysis, a full-length genomic copy of *ABC3* (Figure 1B; 6.3-kb *Hin*dIII fragment) was introduced into the *abc3Δ* strain as a single ectopic integron (Figure 1C). At least two independent strains from each background were examined to assess all the vegetative, reproductive, and pathogenesis-related defects reported here.

When inoculated as mycelial plugs or as conidial suspension on complete agar medium, the *abc3Δ* mutant grew slower (~30% reduction in colony size; $P < 0.05$) than wild-type Guy11 (Figure 3A), although no apparent difference in conidiogenesis or the overall colony morphology was uncovered. However, when crossed to TH3 (*mat1-1*), the *abc3Δ* (*mat1-2*) mutant showed a slight reduction in its sexual reproduction, displaying a decrease in the total number of perithecia produced per sexual cross (Figure 3B). Such defects were not mating-type specific as judged by analyzing the sexual crosses between an *abc3Δ* (*mat1-1*) and wild-type Guy11 (*mat1-2*) (Figure 3B) and could be attributed to reduced female fertility in the *Magnaporthe* strains used (Valent et al., 1991). The complemented *abc3Δ* strain behaved like the wild type in the ability to form perithecia. This suggested a divergence of function for Abc3p compared with the related Ste6 protein, which is required specifically for the efflux of only the a-factor pheromone in *Saccharomyces*. These results indicated that in *Magnaporthe*, the *ABC3* function is required for proper vegetative growth of the mycelia but is dispensable for sexual reproduction. Next, we assessed the germination efficiency and growth of the *abc3Δ* conidia. Conidia produced by the *abc3Δ* strain were normal in quantity, morphology, and germination compared with the wild-type conidia (Figure 3C). Figure 3D shows that upon germination, the *abc3Δ* conidia produced appressoria (average diameter 11.2 ± 0.7 μm; $n = 3000$, $P < 0.05$) that were marginally larger than those produced by the wild-type strain (10.4 ± 0.6 μm; $n = 3000$, $P < 0.05$).

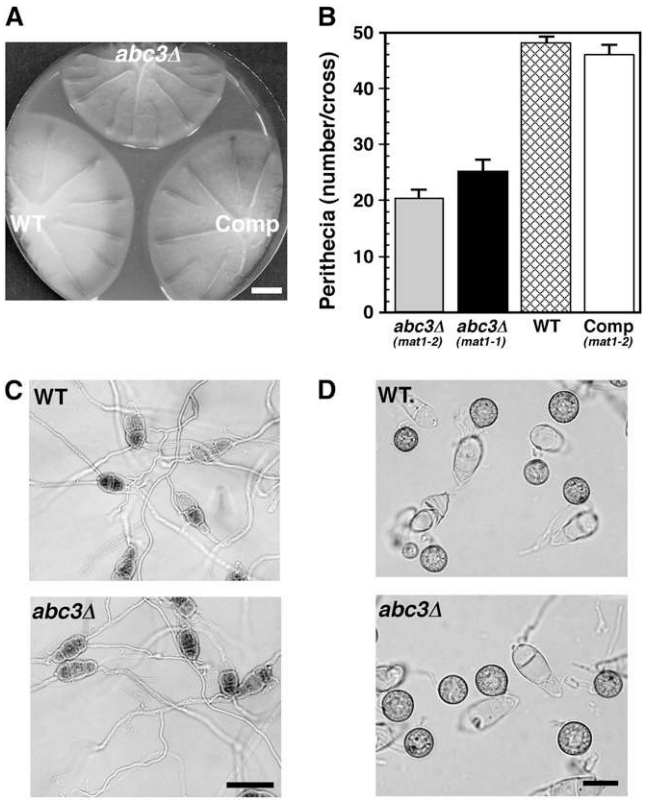

Figure 3. Growth Characteristics and Mating in the *abc3Δ* Mutant.

(A) Wild-type, *abc3Δ*, and an *abc3Δ* strain complemented with the full-length *ABC3* (Comp) were grown on complete medium (CM) for 1 week and photographed. The growth characteristics are representative of three independent assessments (total $n = 27$ colonies per strain; $P < 0.05$). Bar = 1 cm.

(B) Abc3 protein is not required for sexual reproduction in *Magnaporthe*. Perithecia development by the indicated *Magnaporthe* strains in individual sexual crosses with the tester strain of the opposite mating type were assessed 3 weeks after inoculation. Mean values (±SD) represent the number of perithecial beaks observed per mating mix on oatmeal agar medium. Quantifications represent three independent experiments covering a total of 30 crosses per strain. WT refers to the cross between Guy11 (*mat1-2*) and TH3 (*mat1-1*).

(C) Conidia from the wild type or the *abc3Δ* strain were allowed to germinate on CM for 16 h and visualized after acid fuchsin staining. Bar = 20 μm.

(D) The wild type or *abc3Δ* conidia were inoculated on hydrophobic inductive surface (GelBond membrane) and the morphology of the resultant appressoria assessed after 24 h. Bar = 10 μm.

ABC3 Is Essential for *Magnaporthe* Pathogenesis

To assess the role of Abc3p during the host-associated growth and development, we performed infection assays on the seedlings of the rice cultivars CO39 or NIL127 and barley cultivar Express to test the pathogenicity of the *abc3Δ* conidia. The *abc3Δ* mutant (like the TMT2807 strain, Figure 1A) displayed total loss of pathogenicity and failed to elicit any visible blast symptoms/lesions on the compatible (CO39) or incompatible (NIL127) rice varieties when compared with equivalent spray inoculations of wild-type Guy11 conidia or the conidia from the complemented strain (Figure 4A). Under the same conditions, the wild type and the complemented strain caused typical spindle-like, gray-centered, and severe blast lesions that merged into one another on the inoculated rice leaves (Figure 4A). We then quantified the host defense–associated hypersensitive reaction (HR) in the challenged seedlings based on real-time RT-PCR methodology to derive the ratio of rice *Pr-1* to *Actin* gene expression as described by Gilbert et al. (2006). As shown in Figure 4A, the *abc3Δ* mutant failed to elicit proper HR during the compatible or the incompatible interaction with the host. Barley leaf explants challenged with the wild type or the *abc3Δ* mutant for 72 h were costained with 3,3′-diaminobenzidine (DAB) and Trypan blue to visualize the HR symptoms in the challenged tissue. As shown in Figure 4B, the wild-type strain could cause massive damage and cell death and accumulation of reactive oxygen intermediates in the host leaves, whereas the *abc3Δ* mutant failed to elicit any visible HR symptoms in the host and was devoid of such cell death and accumulation of reactive oxygen species, except in rare instances (<1%; arrowhead, Figure 4B; discussed later). To further confirm the lack of HR elicitation, we tested the induction of pathogenesis-related protein 5 (*Pr-5*; Genbank accession number HVU276225) in the barley leaves challenged for 48 h. The ratio of *Pr-5* expression to that of a housekeeping function (*Actin10-4*, Genbank accession number HVU21907) was used to estimate the level of HR induction. In mock inoculations and in barley leaves challenged with the *abc3Δ* mutant, this ratio (*Pr-5/HvAct10*) averaged 1.4 ± 0.3 (over three replicates; $P < 0.05$), whereas the ratio was consistently higher and averaged 2.6 ± 0.5 ($P < 0.005$) when estimated in plants infected by the wild-type fungus. The *abc3Δ* mutant could still be recovered as viable colony-forming units from the challenged leaves but only up to 30 h after inoculation (data not shown). Based on the above plant infection data, we concluded that Abc3p is required for *Magnaporthe* pathogenicity, and upon loss of *ABC3* function, the blast fungus is incapable of establishing disease and eventually fails to survive inside the host.

Since concentrated suspensions of *abc3Δ* conidia failed to elicit any host lesions upon surface inoculation, we decided to test these conidia by two additional means: (1) through inoculation on abraded host leaves and (2) by direct injection of conidia into the leaf nodes or rice leaf sheaths. These assays showed that *abc3Δ* mutant is incapable of causing disease-related host damage even when forcibly introduced through wounded tissue (Figure 4C) or injected directly into the host plants (Figure 4C, bottom panels). Appropriate controls, both positive and negative, were included and are shown alongside in these assays (Figure 4C). Even under such conditions that bypass the requirement of appressorium function, the *abc3Δ* mutant failed to elicit proper HR as judged by the ratio of *Pr-1/Actin* gene expression (Figure 4C).

Rather surprisingly, the mutant appressoria were functional on PUDO-193 cellophane (Clergeot et al., 2001) and penetrated it (Figure 4D, bottom panels), albeit with a much lower efficiency ($39\% \pm 2.5\%$ compared with $58\% \pm 2.1\%$; $P < 0.005$) than the wild-type appressoria. The invasive growth within the cellophane

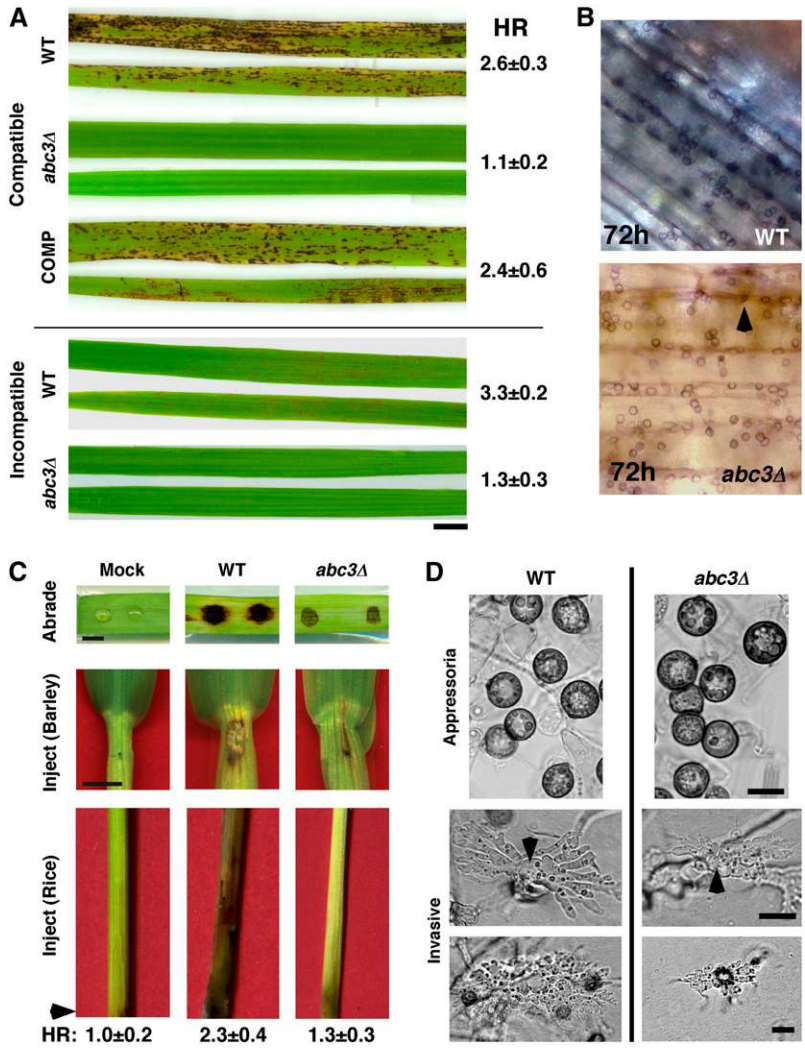

Figure 4. Loss of *ABC3* Function Leads to Nonpathogenicity.

(A) Blast infection assays on host tissue were conducted as follows: rice seedlings belonging to CO39 (compatible) or NIL127 (incompatible) genotypes were spray-inoculated with conidial suspensions (in 0.02% gelatin in water) from the wild type, *abc3Δ* strain, or the *abc3Δ* mutant complemented by the introduction of *ABC3* (Comp), and disease symptoms were assessed after 10 d. Values indicate HR assessed after 48 h and represent the ratio of rice *Pr-1* gene expression to that of the *Actin* transcript. Bar = 1 cm.

(B) The *abc3Δ* strain fails to elicit proper HR-associated host cell death. Barley leaves challenged with the wild type or *abc3Δ* conidia were costained with DAB and Trypan blue to detect peroxide and HR-associated cell death, respectively. Arrowhead depicts the rare HR event in the host upon challenge with the mutant.

(C) Equal number of conidia from the wild type or *abc3Δ* mutant were inoculated either on abraded barley leaves (top panels) or injected at the base of the barley leaves (middle panels) or the base of rice leaf sheaths (bottom panels). Host damage and disease lesion formation were subsequently assessed after 10 d. HR was assessed after 48 h as described in **(A)**. Mock refers to the same inoculation treatments but with a 0.02% gelatin solution devoid of conidiospores. Bars = 0.5 cm.

(D) Mutant *abc3Δ* appressoria are capable of breaching thin cellophane membranes. Equivalent number of conidia from the wild type or the *abc3Δ* mutant were inoculated on synthetic membranes (PUDO-193 cellophane; see Materials) and assessed for germination, appressoria formation, surface penetration, and invasive growth (arrowheads). Bars = 10 μm.

appeared to be compromised in the *abc3Δ* strain. Taken together, we conclude that the *abc3Δ* mutant is incapable of eliciting proper HR or causing blast disease in the host plants but, although inefficiently, is still capable of breaching and invading cellophane membranes.

Genetic Complementation of TMT2807 and the *abc3Δ* Mutant

We introduced pFGLr2 (carrying the full-length *ABC3* gene) or pBarKS (control) into the *abc3Δ* strain and the TMT2807 mutant. Twenty bialaphos-resistant transformants were screened by

DNA gel blot analysis in each instance. Two strains that carried single-copy integration of the *ABC3* gene at an ectopic site in each background (TMT2807 and *abc3Δ*) were used to analyze the suppression of the various phenotypic defects observed in the *abc3Δ* mutant. The mild reduction in vegetative growth and mating efficiency observed in the *abc3Δ* strain (and TMT2807) was completely suppressed upon introduction of the wild-type *ABC3* gene (Figures 3A and 3B, Comp), which also restored its ability to penetrate the host and cause blast disease (Figure 4A, COMP). The complemented strain was found to be as virulent as the wild-type isolate when spray-inoculated on rice seedlings (Figure 4A, COMP). By contrast, the vector control could not suppress these abnormalities (data not shown). Since all the defects in the *abc3Δ* mutant (and TMT2807) could be completely restored by reintroduction of the wild-type *ABC3* allele, we conclude that the phenotypic changes and functional abnormalities observed in the *abc3Δ* strain resulted solely from the disruption of *ABC3* function.

Infection Structure–Related Defects in *abc3Δ*

Next, we addressed the question whether the ability to breach the artificial membranes but not the host tissue was due to a decrease in appressorial turgor in the *abc3Δ* strain. We therefore estimated the appressorial turgor through the incipient cytorrhysis assays (Howard et al., 1991; de Jong et al., 1997). Such appressorial collapse assays (Table 1) revealed that compared with the wild type, the *abc3Δ* mutant displayed a slightly lower appressorial turgor, although not statistically significant. This reduction in turgor in the mutant appressoria was particularly evident when the external glycerol addition was in the molar range of 3.5 to 4.5. At lower molar concentrations (1 to 3 M), the internal turgor levels were inferred to be equivalent to those estimated in the wild-type appressoria. As judged by light microscopy and by thin-section transmission electron microscopy (TEM), melanin deposition appeared wild type–like in the *abc3Δ* appressoria. We isolated TMT2807 and the *abc3Δ* strain as totally nonpathogenic mutants incapable of causing blast disease or host damage (Figures 1A and 4). Therefore, we performed detailed microscopic analyses of the infection cycle to determine which stage of the pathogenesis process was compromised in the *abc3Δ* strain. Quantitative appressorium formation assays using conidia from the wild type or *abc3Δ* revealed that the ability to germinate and form appressoria on barley leaf or onion epidermal strips or rice leaf sheath was not affected in the mutant (Figure 5A). However, a striking difference was that compared with the wild type, only a negligible percentage of *abc3Δ* appressoria (0.7% ± 0.9%; $n = 3000$, over three replicates) could produce penetration pegs as judged by aniline blue staining for papillary callose deposits and infection hyphae formation (Figures 5A to 5C; 48 h). In the wild type, the ability to form penetration pegs on barley leaves was ~83% (± 2.9; $n = 3000$) at the equivalent 48-h time point. Even upon extended incubation, the failure to penetrate the host surface remained unchanged (Figure 5C, 72 h). Even 96 h after inoculation, a vast majority of the *abc3Δ* appressoria (~99%) still failed to enter the host and to elicit callose deposition (data not shown). By contrast, the resultant wild-type infectious hyphae within the host (Figures 5B and 5C) were already in their ramifying and proliferating stage in planta.

To further validate our findings above, we used thin-section TEM-based ultrastructural analysis to ascertain whether *abc3Δ* appressoria were indeed defective in host penetration. Such TEM analysis confirmed that the majority of the *abc3Δ* appressoria failed to penerate the host surface and did not elicit any visible reaction from the plant (Figure 6A, *abc3Δ*, 48 h). We could detect futile attempts at penetration in only two appressoria (out of 142 appressoria sectioned) in *abc3Δ* (Figure 6A, 72 h). In each instance, the dense papillary callose deposits obstructing the site of failed entry were clearly visible (Figure 6A). The TEM sections for the wild-type appressoria depicted the successful penetration and elaboration of typical fungal infectious hyphae in the host tissue (Figures 6A and 6B, rice sheath assay). The *abc3Δ* mutant failed to elaborate any infection hyphae in barley, onion (*Allium cepa*), or rice (Figure 6C). Based on these results, we conclude that a defect in appressorium-mediated host penetration leads to nonpathogenicity in mutants lacking the *ABC3* function. Taken together, we construe that Abc3p plays an extremely important role in the host penetration step of disease establishment and is probably also required for the in planta spreading of the blast fungus.

In addition, *abc3Δ* was incapable of surviving the host environment since viable *abc3Δ* cultures could not be recovered from the penetration assays and the wounding assays beyond 30 h after inoculation. Quantitative cell-viability assays using Phloxine B (which accumulates in dead cells) showed that the *abc3Δ* mutant was incapable of surviving the environment encountered within the host irrespective of the mode of entry (Figure 7A; surface inoculation or injection). Appressorial assays on cellophane revealed that viability and invasive growth is significantly compromised in the mutant (Figure 7A, 48 h; $P < 0.05$). Moreover, addition of barley leaf extract during appressorial assays on cellophane caused a further and marked reduction in the viability of the mutant therein (Figure 7A, 48h+Extr). The wild-type strain remained largely unperturbed under these conditions. We conclude that the *ABC3* function plays a critical role during early stages of disease establishment and is most likely required for the in planta viability and survival of the blast fungus.

Table 1. Appressorial Cytorrhysis Assay in Wild-Type Guy11 and *abc3Δ*

External Glycerol (Molar Concentration)	Guy11 Cytorrhysis (%)[a]	*abc3Δ* Cytorrhysis (%)[a]
1.0	5.0 ± 1.1	6.2 ± 1.5
2.0	8.2 ± 0.9	10.0 ± 1.7
3.0	32.0 ± 0.8	33.0 ± 1.0
3.5	63.0 ± 1.1	68.1 ± 1.4
4.0	81.5 ± 1.7	85.1 ± 1.2
4.5	85.0 ± 0.8	89.2 ± 1.1

[a] Refers to the mean (±SD) of three independent estimations, each involving 10^3 appressoria ($P < 0.05$). The appressoria were allowed to form for 45 h on GelBond membrane prior to the addition of the indicated concentration of external glycerol.

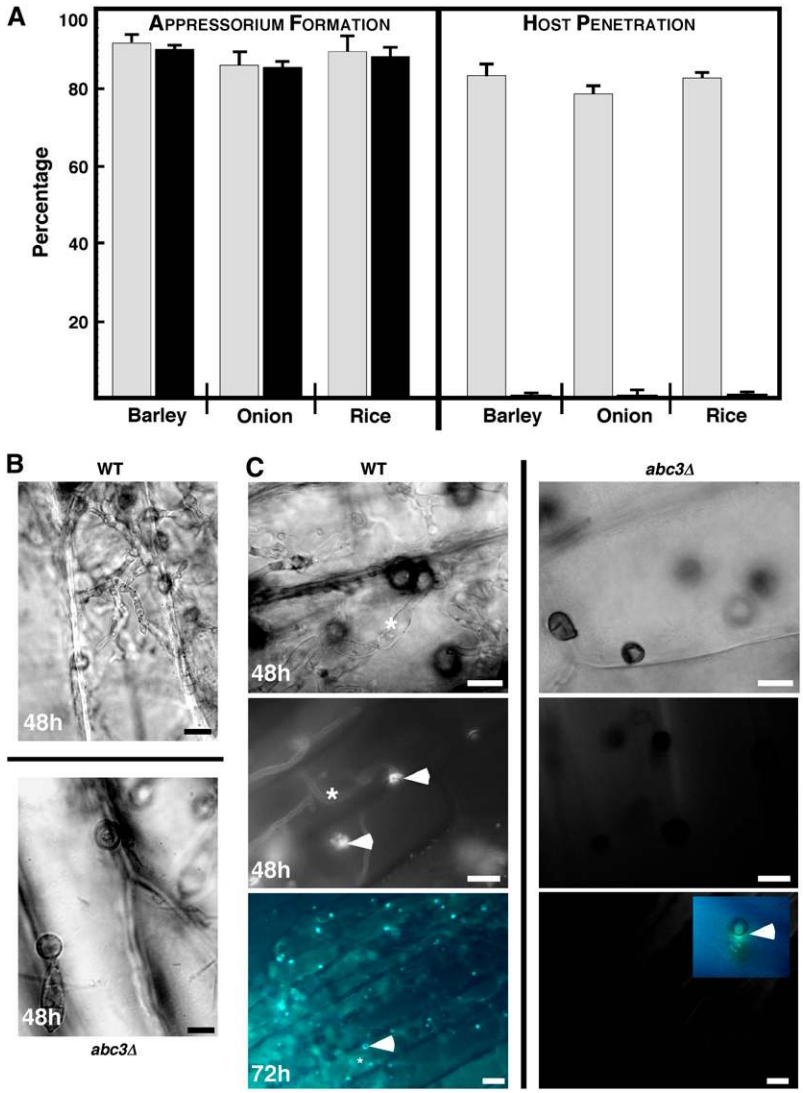

Figure 5. Appressorium Function and Host Penetration Defects in the *abc3Δ* Strain.

(A) The *abc3Δ* appressoria are incapable of appressorium function. Equal number of conidia from the wild-type strain (gray bars) or the *abc3Δ* mutant (black bars) were inoculated on barley leaf explants, onion epidermal strips, or rice leaf sheaths and assessed in each instance for appressorium formation (at 24 h) and appressorium function (host penetration and invasion, as judged by aniline blue staining of resultant callose deposits at 48 h). Values are mean ± SD from three replicates of the experiment, each involving 10^3 conidia.

(B) and **(C)** Loss of appressorium function of plant penetration in the *abc3Δ* mutant. Equal number of wild-type or *abc3Δ* conidia were inoculated on onion epidermal strips **(B)** or barley leaf explants **(C)** and allowed to proceed through infection-related development for the indicated time. The papillary callose deposits (arrowheads; see **[A]** for quantifications) and infection hyphae (asterisk) were visualized after staining the barley leaf explants with aniline blue at 48 h (top panels) or 72 h (bottom panel) after inoculation. The inset depicts the rare papillary callose deposit (arrowhead) produced by the *abc3Δ* appressoria. Bars = 10 μm.

Abc3p and MDR

Earlier studies have documented the role of MDR P-glycoproteins in the efflux of a diverse range of compounds, such as steroid hormones (Uhr et al., 2002), mating pheromone (Ketchum et al., 2001), drugs and antibiotics (Nishi et al., 1992), and extrusion of ions or solutes (Kimura et al., 2005). To test whether Abc3p serves similar extrusion function(s), we investigated the drug sensitivity of the *abc3Δ* strain. We tested the effect of metabolic poisons, antifungal agents, and antibiotics on *abc3Δ* strain and wild-type Guy11. As shown in Table 2, sensitivity to each compound was determined as the minimum inhibitory concentration of that compound required for inhibiting mycelial growth in wild-type Guy11. Among the drugs tested, *abc3Δ* strain showed increased sensitivity to valinomycin and actinomycin D. The MDR correlated with the function of an ABC or

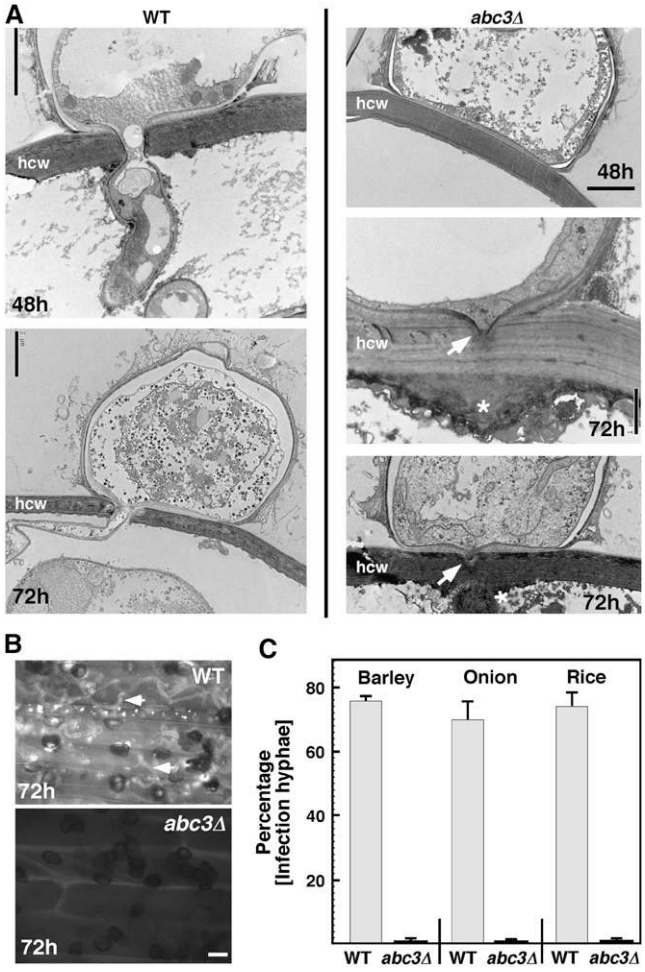

Figure 6. The *abc3Δ* Mutant Fails to Penetrate and Colonize the Host.

(A) Barley leaves were challenged with conidia from the wild type or *abc3Δ* and processed for thin-section TEM at the indicated time points after inoculation. Near-median TEM sections were selected for assessment and are represented here. Arrows indicate the nonfunctional penetration pegs elaborated by *abc3Δ* appressoria, whereas the callose deposits are marked by an asterisk. hcw, host cell wall. Bar = 2 μm, except for the middle right panel where it denotes 1 μm.

(B) The *abc3Δ* strain fails to produce infection hyphae. Conidia from the wild type or *abc3Δ* were inoculated on barley leaf explants, onion epidermal strips, or rice leaf sheaths (processed for aniline blue staining after 72 h). Arrow indicates the infection hyphae within the leaf sheath tissue.

(C) Respective quantifications of the infection hyphae from three independent experiments in each instance, where values (±SD) are indicated as percentage points.

P-glycoprotein transporter since it could be reversed by the presence of verapamil (Table 2) in Guy11. Our minimum inhibitory concentration assays did not show any difference in the sensitivity of Guy11 and *abc3Δ* mutant for the other compounds tested, such as brefeldin A, gramicidin D, leptomycin B, benomyl, and some azole fungicides.

Having confirmed an important efflux-related role of Abc3p during the mycelial growth phase of *Magnaporthe*, we then assessed whether Abc3p is also required during the pathogenic phase for a similar MDR function. As shown in Figure 7B, the germ tube growth from *abc3Δ* conidia was inhibited upon valinomycin treatment, whereas the germ tube growth in Guy11 could withstand an elevated concentration of valinomycin (20 μg/mL). On proper inductive surfaces, the wild-type conidia germinated and formed appressoria in the presence of valinomycin, albeit at a lower frequency: 61 ± 2% versus untreated wild-type samples, where the rate of appressorium differentiation was found to be 93% ± 5% (Figure 7C). The appressoria formed under these conditions were also substantially smaller. By contrast, the same concentration of valinomycin had a very severe and dramatic effect on the conidia of the *abc3Δ* mutant: a complete blockage of conidial germ tube emergence (Figure 7C). It has been proposed that valinomycin can also affect the homeostasis of potassium ions across biological membranes (Daniele and Holian, 1976). However, exogenous addition of potassium chloride did not suppress the effect of valinomycin toward the conidia and appressoria of neither the wild type nor the *abc3Δ*. We conclude that the Abc3 protein serves an essential multidrug resistance function both during the vegetative and the pathogenic phases of the rice blast fungus and suggest that such MDR activity is most likely directed toward compounds related to valinomycin in their structure and/or properties. Abc3p could also functionally replace its ortholog, Pmd1p, from fission yeast (Figure 7D), signifying the evolutionary conservation and importance of such MDR phenomenon.

Abc3p and Sensitivity to Cellular Stress

Since addition of potassium could not reverse the effect of valinomycin, we reasoned that the Abc3 protein functions through some as yet unknown mechanism to modulate its MDR activity toward such antifungal compounds. We therefore investigated whether Abc3p is required for modulating osmotic, oxidative, and/or related cellular stress conditions. Compared with the wild-type strain, *abc3Δ* mutant did not show a difference in its mycelial growth in high concentrations of osmolytes, such as sorbitol or sucrose, or sodium chloride. By contrast, the *abc3Δ* mutant was found to be highly sensitive to oxidative stress, and even a small dose (2 mM) of hydrogen peroxide was found to be lethal to the mutant strain (Figure 8A), whereas the wild-type Guy11 strain remained unperturbed under such adverse growth conditions (Figure 8A). The *abc3Δ* mutant also showed similar sensitivity to paraquat and menadione, which stimulate accumulation of reactive oxygen species/intermediates (ROS; data not shown). The sensitivity of the *abc3Δ* mutant to such oxidative stress was common to the vegetative and pathogenic growth phases (Figure 8B). Nitroblue tetrazolium–assisted visualization of the accumulation of reactive oxygen radicals in the wild type and the *abc3Δ* colonies showed that the mutant hyphae accumulated relatively higher amounts of peroxide and likely a higher amount of ROS (Figure 8C; the dark centers in the wild-type colony are due to the enhanced contrast of the image). Such increased accumulation of peroxides/DAB-positive material was also detected in the *abc3Δ* mutant

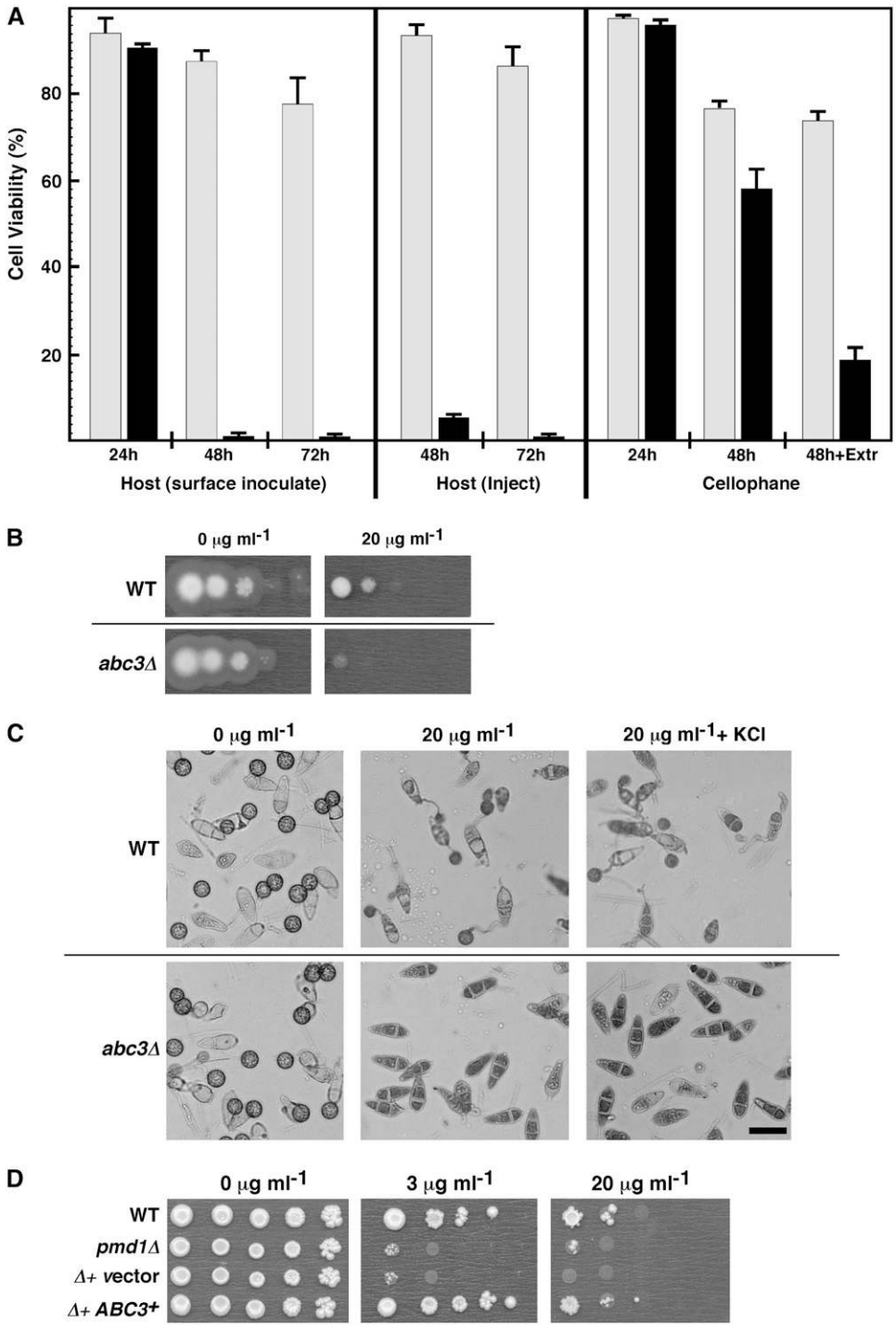

Figure 7. Decrease in Cell Viability and MDR Function in the *abc3Δ* Strain.

(A) Conidia from the wild type (gray bars) or the *abc3Δ* strain (black bars) were inoculated on barley leaves (host; either by surface inoculation or injection method) or cellophane membrane and allowed to undergo pathogenic development. Cell viability was quantified at the indicated time points by staining with phloxine B. Values represent mean ± SD from three experiments. A parallel experiment included viability counts during appressorium development and penetration of cellophane in the presence of water-soluble extracts from barley leaves for 48 h (48h+Extr).

(B) and **(C)** Abc3 protein serves an essential MDR function during vegetative and pathogenic growth. Equivalent serial dilutions of conidial suspensions from the wild type or *abc3Δ* were cultured in the presence (20 μg/mL) or absence (0 μg/mL) of valinomycin on complete growth medium **(B)** for 5 d or on artificial inductive membranes **(C)** for 36 h. Addition of potassium (KCl at 100 mM) fails to reverse the defects associated with valinomycin action on *Magnaporthe* condiospores and appressoria. Bar = 15 μm.

(D) *ABC3* rescues the valinomycin sensitivity associated with the loss of orthologous *pmd1*$^+$ locus in *Schizosaccharomyces pombe*. Fission yeast strains belonging to the relevant genotypes (as specified) were cultured on YES medium in the absence or presence of the indicated amounts of valinomycin. Results were documented 5 d after inoculation. Strain Δ+ vector refers to the *pmd1Δ* mutant carrying an empty plasmid vector, whereas Δ+ *ABC3*$^+$ denotes the *pmd1Δ* mutant expressing an integrated copy of the *ABC3* gene.

Table 2. Drug Sensitivity of Wild-Type Strain Guy11 and *abc3Δ*

Compound	Guy11	*abc3Δ*
Valinomycin	20 μg/mL	3 μg/mL
Valinomycin + verapamil	10 μg/mL	3 μg/mL
Actinomycin D	15 μg/mL	3.5 μg/mL
Actinomycin D + verapamil	8 μg/mL	3.5 μg/mL
Benomyl	2 μg/mL	2 μg/mL
Brefeldin A	40 μg/mL	40 μg/mL
Gramicidin D	180 μg/mL	180 μg/mL
Leptomycin B	7.5 ng/mL	7.5 ng/mL
Fluconazole	2.5 μg/mL	2.5 μg/mL
Itraconazole	2 μg/mL	2 μg/mL

Drug sensitivity is determined as the minimum inhibitory concentration that is sufficient to inhibit growth of *Magnaporthe* mycelia on agar medium.

appressoria on artificial membranes and barley leaf explants (Figure 8D, bottom panels). Fluorimetric evaluation of hydrogen peroxide levels in the wild type and *abc3Δ* on barley leaves, after staining with the dye chloromethyl-2′,7′-dichlorofluorescein diacetate (CM-DCFDA), revealed that the mutant appressoria accrue 3.5-fold higher amounts of ROS/peroxide than those estimated in the wild type (Figure 8E). An earlier study has shown that oxidative stress (accumulation of DAB-positive material) precedes the elicitation of cell death in the interacting epidermal cells and the underlying mesophyll cells in *Brachypodium* infected with *Magnaporthe* (Routledge et al., 2004).

To understand whether the pathogenicity defects in *abc3Δ* are in any way related to the excess buildup of H_2O_2 therein, we tried to reduce the levels of peroxide oxidants during appressorium development using several agents, such as 15 μm diphenyleneiodonium,10 μm nordihydroguaiaretic acid, 5 μm rotenone (Chiarugi et al., 2003), or antioxidants (ascorbate or *N*-acetylcysteine). The addition of diphenyleneiodonium could partially (in 5.1% ± 1.1% appressoria; $n = 3000$) suppress the host penetration defects associated with the *abc3Δ* appressoria (Figure 9A). However, antioxidant treatment with either ascorbate or *N*-acetylcysteine restored penetration function in 23% ± 2.5% and 19% ± 1.6% appressoria, respectively (Figure 9A; $n = 3000$, $P < 0.005$), as judged by papillary callose deposition. However, the resultant mutant penetration pegs still failed to elaborate proper infection hyphae and were unable to advance the invasion further (data not shown). We conclude that reduction of the intracellular peroxide levels (or oxidative stress) in *abc3Δ* leads to a significant suppression of the appressorial defects in this mutant.

In a converse experiment, we tested the effect of exogenous hydrogen peroxide, menadione, or paraquat on the ability of the wild-type appressoria to penetrate the host surfaces. As expected, in the absence of exogenous peroxide, the wild-type appressoria behaved normally and were able to successfully penetrate the host surface as judged by papillary callose deposits upon aniline blue staining. In this instance, the percentage of appressoria that elaborated penetration pegs was 68% ± 2.3% ($n = 3000$ apppressoria, over three replicates), after the 48-h time point. Addition of 3 mM peroxide to the wild-type conidia caused a significant decrease in host penetration with only 36% ± 2.8% appressoria (Figure 9B; $n = 3000$, over three replicates) able to breach the host surface. Addition of paraquat or menadione had a slightly reduced effect on host penetration of the wild type compared with treatment with peroxide (Figure 9B). Such oxidative stress caused a significant reduction in the efficiency of appressorium formation (Figure 9B), and peroxide levels exceeding 5 mM blocked germ tube emergence in the wild-type conidia (data not shown). A verapamil-based general downregulation of MDR activity during pathogenic development showed a significant decrease (maximal 74%) in penetration peg formation but without affecting the germ tube emergence or growth. On the basis of these results, we conclude that excessive peroxide levels have an adverse effect on the host penetration capacity of *Magnaporthe* and construe that reducing the intracellular levels of peroxide (or oxidative stress) in *abc3Δ* significantly suppresses the appressorial defects observed in this mutant. Taken together, we conclude that Abc3p performs an important MDR function during pathogenic phase and possibly protects the blast fungus from peroxide-based internal oxidative stress during vegetative and pathogenic development.

abc3Δ Appressoria Accumulate Toxic Metabolite(s)

Since Abc3p was predicted to be an MDR protein, it raised an attractive possibility that the *abc3Δ* appressoria possibly retain cytotoxic molecule(s) that block the appressorial function of elaborating penetration pegs. To address this issue, we prepared intracellular and extracellular extracts (see Methods for details) from the appressoria of the wild type or the *abc3Δ* strain and used these extracts individually during plant infections with the wild-type conidia. The said extracts were added to the wild-type conidia in barley leaf infection assays at 0 or 23 h after inoculation. A solvent control at the equivalent concentration was included. The intracellular extract from the *abc3Δ* appressoria, when added at the start of the wild-type infection, caused a dramatic (~74%; $P < 0.005$) reduction in penetration peg formation, as judged by aniline blue staining for papillary callose deposits (Figure 10A, 0 h). There was no decrease whatsoever in the appressorium formation capability under these conditions. The corresponding extract from the wild-type appressoria resulted only in a slight decrease (~24%) in host penetration. This decrease by the wild-type extract was comparable to the reduction observed when either the wild type or the mutant extract was added after the infection had proceeded for 23 h (Figure 10A, 23 h). The control extracts did not cause any significant decrease in the host penetration capability of the wild-type appressoria (Figure 10A) and neither did the extracellular extracts from the wild type or the *abc3Δ* appressoria (data not shown). These results lead us to hypothesize that the *abc3Δ* mutant is unable to efflux certain toxic or inhibitory metabolites, whose accumulation in the mutant appressoria likely inhibits host penetration.

Next, we tested the ability of the intracellular extract from *abc3Δ* appressoria to suppress penetration of artificial substrates by the wild type or the mutant. We therefore performed wild-type and *abc3Δ* appressorial assays on PUDO-193 cellophane in the presence or absence of this extract. As shown in Figure 10B, addition of the intracellular *abc3Δ* extract caused a significant reduction

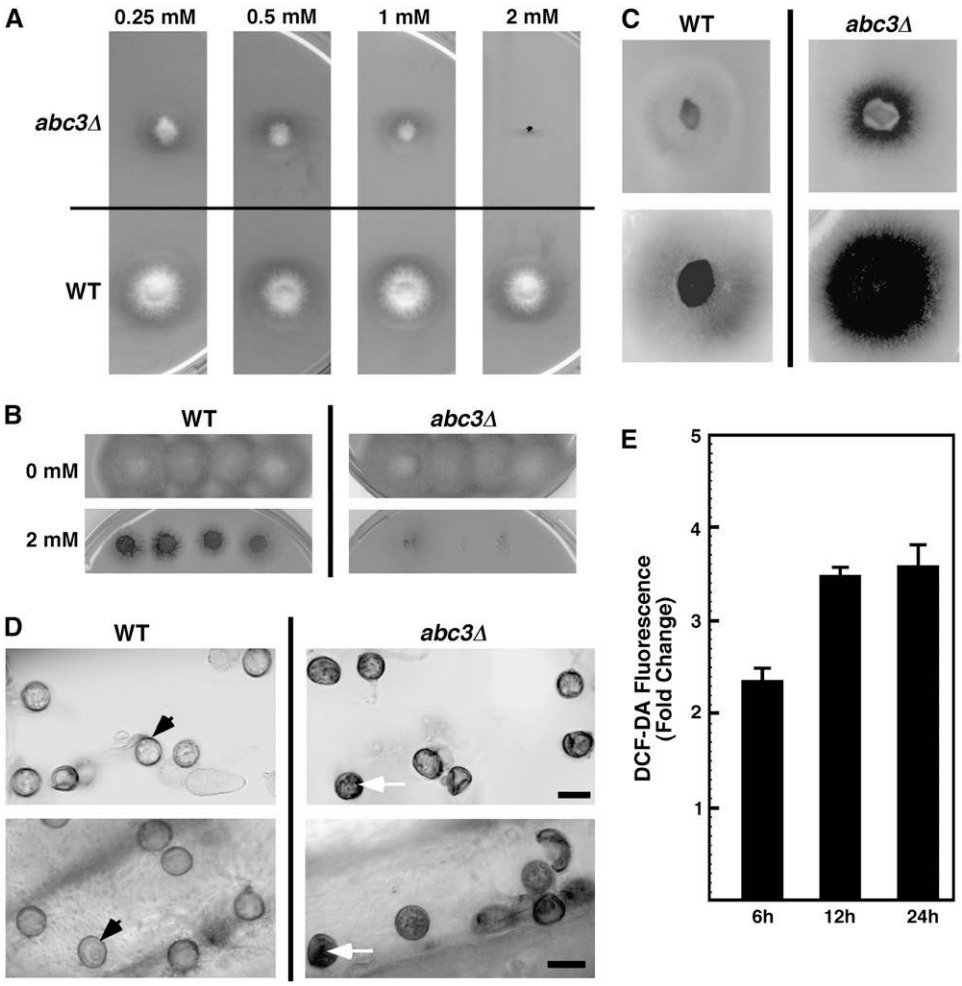

Figure 8. *abc3Δ* Is Highly Sensitive to Oxidative Stress and Accumulates Excess Peroxide and Reactive Oxygen Intermediates.

(A) and **(B)** Mycelial plugs **(A)** or equivalent serial dilutions of conidiospore suspensions **(B)** from the *abc3Δ* strain or the wild type were cultured on minimal agar medium containing the indicated amounts of hydrogen peroxide. The results were documented after an incubation period of 1 week.

(C) The *abc3Δ* strain accumulates excess peroxide. Three- (top panels) or six-day-old (bottom panels) wild-type or *abc3Δ* colonies were stained with nitroblue tetrazolium solution to detect peroxide accumulation.

(D) Peroxide accumulation during pathogenic phase. In vitro and in vivo DAB reactions. Wild-type and *abc3Δ* appressoria formed on artificial membranes (top panels) or on barley leaf explants (bottom panels) were stained with DAB to detect the accumulation of hydrogen peroxide (black arrows). White arrows indicate the excess DAB-reactive deposits within the appressorial lumen. Bars = 10 μm.

(E) Total extracts from the wild type or the *abc3Δ* appressoria were treated with CM-DCFDA and processed for fluorimetric estimations. Values in the graph represent fold change (mean ± SD; from three independent experiments) in the CM-DCFDA–reactive material from mutant appressorial extracts compared with those in the wild type. Average value for the CM-DCFDA estimates in the wild-type extracts was set at 1.

(~85% in the wild type and 89% in *abc3Δ*; $P < 0.005$) in appressorium function on cellophane membranes. Surprisingly, the intracellular *abc3Δ* extract showed minimal effect on the viability of the wild type or the *abc3Δ* mycelia (Figure 10C). Interestingly, when included during blast infection assays, the intracellular *abc3Δ* extract caused a dosage-dependent and noticeable reduction in the elaboration of disease symptoms on rice leaves (Figure 10D). The said mutant extract also caused an elicitation of visible HR-like symptoms as judged by the occurrence of brown lesions (in the absence of fungal biomass) in treated samples and inferred by the measurement of the ratio of rice *Pr-1* to *Actin* gene expression (Figure 10D; $P < 0.05$). We conclude that Abc3p is important for the efflux of certain appressorial metabolites, whose accretion has a negative effect on host penetration.

Regulation of *ABC3* Expression

Given the above findings that showed the involvement of Abc3p in regulating oxidative stress within the fungal cellular structures, we decided to test whether such stress conditions directly influence *ABC3* expression. To this end, we performed a qualitative and quantitative study of *ABC3* expression during the

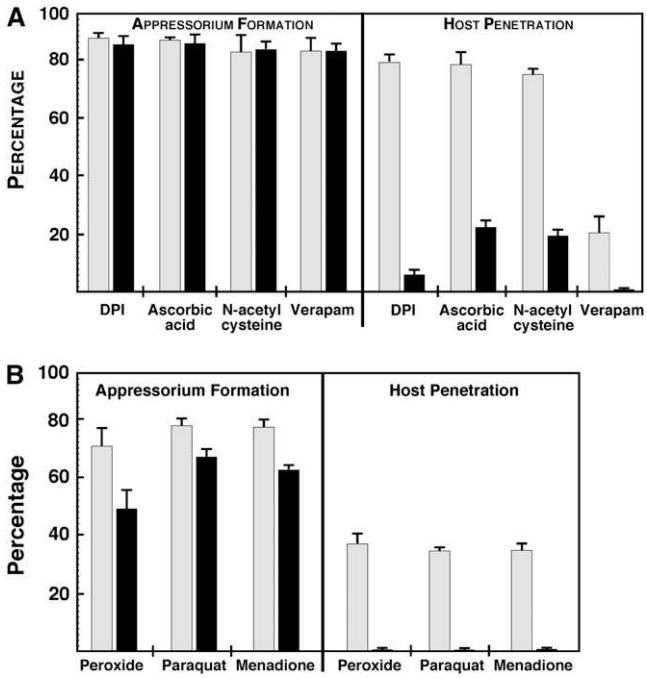

Figure 9. Partial Suppression of *abc3Δ* Defects and Effect of Verapamil and Oxidative Stress.

(A) Antioxidant treatment restores appressorium function partially in *abc3Δ*. Wild-type (gray bars) or *abc3Δ* (black bars) conidia were tested for appressorium formation and function (host penetration) on barley leaf explants in the presence of diphenyleneiodonium (DPI), ascorbate, or *N*-acetylcysteine. The above experiment was also performed in the presence of verapamil (Verapam), a generic inhibitor of MDR-based efflux functions. The treatments were performed for 48 h in each instance and host penetration assessed by aniline blue staining. Values represent mean ± SD from three independent experiments, each involving 2000 conidia per strain.

(B) Exogenous addition of oxygen radical producing agents reduces appressorium function in the wild type. Conidia from the wild-type (gray bars) or the *abc3Δ* strain (black bars) were inoculated on barley leaf explants in the presence of either hydrogen peroxide, paraquat, or menadione and the resultant appressorium formation and function (host penetration) assessed after 48 h as described above. Values represent mean ± SD from three independent experiments, each involving 2000 conidia per strain.

infection-related developmental stages of two independent transformants, each carrying a single-copy destabilized green fluorescent protein (deGFP) reporter driven by the *ABC3* promoter. As shown in Figure 11A, the destabilized GFP fluorescence increased dramatically upon treatment with hydrogen peroxide. The fluorescence intensification was found to be fourfold higher compared with that assessed in the untreated control samples (data not shown) and was maximal after a 9-h treatment (Figure 11A). Low levels of paraquat or valinomycin elicited a similar increase in the *ABC3* promoter-driven destabilized GFP expression (data not shown) during appressorium development. Based on these results, we concluded that the upstream regulatory elements of the *ABC3* gene respond to the model molecules that generate reactive oxygen radicals and that the *ABC3* transcript is likely regulated in a redox-responsive manner during infection-related development in *Magnaporthe*.

To study whether *ABC3* expression is also governed by host signals, we performed semiquantitative RT-PCR (Soundararajan et al., 2004) analysis of total RNA extracted at various time intervals from barley leaves challenged with wild-type conidia. Along with *ABC3*, we included *TUB1* (β-tubulin) and Mg *CHAP1* as controls. *CHAP1* transcript has been shown to be under redox regulation in *Cochliobolus* (Lev et al., 2005). As shown in Figure 11B, the highly abundant *TUB1* showed hardly any difference in its expression during the duration of the assay. *ABC3* expression was always weaker compared with *TUB1* but showed an induction at the 18- to 20-h stage after inoculation. Its expression remained stable and strong after the induction at this time point and continued to be so up to 36 h after inoculation (Figure 11B). *CHAP1* expression also peaked at 12 to 18 h but declined slightly after the 24-h time point. Taken together, we conclude that the *ABC3* promoter responds positively to the redox status of the cell and that the *ABC3* gene expression is likely influenced by the host signals too, with an induction just before the fungus readies itself to enter the host tissue.

Subcellular Localization of GFP-Tagged Abc3p

The predicted secondary structure of Abc3p suggested that it is an integral membrane protein with 12 transmembrane helices. To determine the distribution pattern of Abc3p within the various cell types in *Magnaporthe*, the *ABC3-GFP* fusion construct was introduced into the Guy11 strain. Two transformants carrying a single copy of the *ABC3:GFP* allele tagged at the genomic locus and two control strains were identified by requisite PCR analyses and further confirmed by DNA gel blot and protein gel blot analyses (data not shown). GFP detection was performed by either epifluorescence microscopy or using confocal laser scanning fluorescence microscopy. Compared with the wild type, strains expressing Abc3-GFP showed no obvious difference in growth or pathogenesis, suggesting that Abc3-GFP is fully functional. Abc3-GFP was adjudged to be a plasma membrane resident protein based on the distinct green fluorescence in the mycelial outer membranes (Figure 12A). No detectable GFP signals were observed in the conidia of the *ABC3:GFP* strain (Figure 12A), although the germ tubes showed a faint GFP signal in the plasma membrane (data not shown). A time-course analysis during appressorium development and maturity suggested that the Abc3-GFP protein was highly expressed and concentrated in the appressorial plasma membrane right from the incipient stage onwards (Figure 12B). However, at a later stage (17 h after germination) during the appressorium maturation, Abc3-GFP signal was predominantly found in the vacuolar compartments as well (Figure 12B, 20 h), although the plasma membrane residency was diminished substantially. Colocalization studies to confirm vacuolar residency involved staining with LysoTracker Red DND-99 or with Neutral Red (Figure 12C, vacuoles). Continuing further, the Abc3-GFP localization during host penetration and invasive growth revealed that Abc3-GFP localized to the plasma membrane of the newly formed penetration hyphae (Figure 12D) but was undetectable in the resultant infection hyphae. Consistent with its role in appressorium

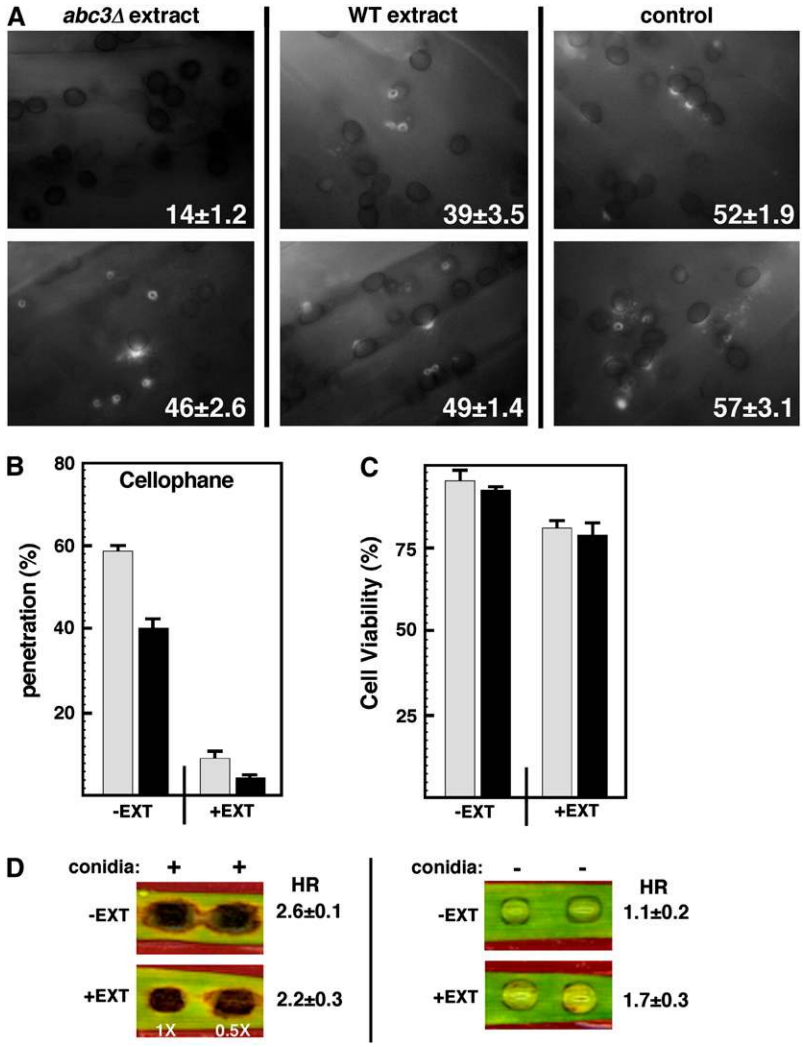

Figure 10. The *abc3Δ* Appressoria Accumulate Inhibitory Molecule(s) Capable of Blocking Penetration Peg Formation.

(A) Intracellular neutral extract prepared from the appressoria of the wild type or the *abc3Δ* strain was used during plant infections with the wild-type conidia. The said extracts were added to the wild-type conidia in barley leaf infection assays at 0 h (top panels) or 23 h (bottom panels) after inoculation. A solvent control at the equivalent concentration was included (control) in parallel. Values indicate penetration efficiency (mean values as percentage points ± SD from three replicates) calculated after 48 h by staining papillary callose deposits with aniline blue.

(B) The intracellular neutral extract from *abc3Δ* inhibits appressorium-mediated penetration of cellophane membranes. Wild-type (gray bars) or *abc3Δ* (black bars) conidia were inoculated on PUDO-193 membrane and assessed for appressorium function in the absence (-EXT; solvent control) or presence (+EXT) of the intracellular neutral extract from the *abc3Δ* mutant. Values represent mean ± SD from three replicates of the experiments.

(C) Cell viability was assessed with phloxine B staining in vegetative mycelia from the wild type (gray bars) or *abc3Δ* (black bars) in the absence (-EXT; solvent control) or presence (+EXT) of the intracellular neutral extract from the *abc3Δ* appressoria.

(D) The intracellular extract from the mutant elicits mild HR and reduces blast disease symptoms. Wild-type conidia were tested in barley leaf inoculation assays in the absence (-EXT; solvent control) or presence (+EXT; at 1× or 0.5× concentration) of the above-mentioned extract from *abc3Δ*. A parallel experiment was performed in the absence of conidia. Blast symptoms were assessed and documented 5 d after inoculation, whereas the HR (mean values ± SD of rice *Pr-1*/*Actin* ratio from three independent experiments; $P < 0.05$) was estimated at 48 h after inoculation.

function and its localization pattern described above, we conclude that *Magnaporthe* Abc3p is a transmembrane protein found in the mycelia and predominantly in the appressoria, where we speculate, it is most likely required for the efflux of toxic metabolite(s) and/or for regulating the oxidative stress within these highly important fungal infection structures.

DISCUSSION

Isolation and Molecular Analysis of the TMT2807 Mutant

We isolated TMT2807 as a nonpathogenic mutant in *Magnaporthe*. Molecular genetics and further characterization of TMT2807 helped identify the MDR P-glycoprotein encoding

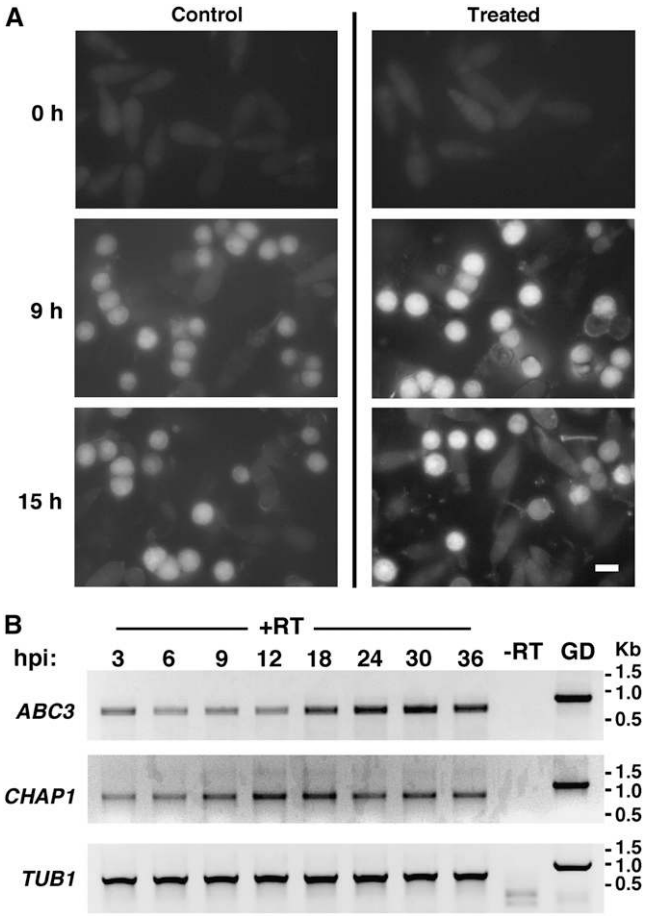

Figure 11. Redox-Responsive and Host-Dependent Regulation of *ABC3* Expression.

(A) Conidia from the *ABC3(p)*:*deGFP* strain were allowed to undergo appressorium development for 24 h in the absence (Control) or presence (Treated) of 1 mM H_2O_2. Epifluorescent microscopic observations were performed at the indicated time points to detect destabilized GFP expression driven by the *ABC3* promoter. Bar = 10 μm.

(B) Host surface–dependent regulation of *ABC3* transcript levels. Semi-quantitative RT-PCR–derived products amplified using *ABC3*-, Mg *CHAP1*-, or Mg *TUB1*-specific primers from total RNA extracted from the wild-type strain grown for the indicated hours after inoculation (hpi) on barley leaves. Negative control (-RT) refers to the RNA sample being processed without a reverse transcriptase step prior to the PCR amplification. GD refers to the PCR amplification of the respective fragments from the genomic DNA samples using the corresponding primer sets. Molecular mass standards (in kilobase pairs) are shown.

gene *ABC3* as a novel pathogenicity factor in *Magnaporthe*. To confirm the role of Abc3p in *Magnaporthe* pathogenesis, we created and characterized *abc3Δ* mutants in two separate wild-type backgrounds, namely, Guy11 and B157. Such studies clearly demonstrated that loss of Abc3p in *Magnaporthe* leads to a complete loss of pathogenicity toward rice and barley. The *abc3Δ* colonies were slow growing compared with the wild type but were largely unaffected in morphology and in conidia formation. Genetic complementation analyses confirmed that the defects seen in TMT2807 and *abc3Δ* were due solely to the loss of *ABC3* function in these mutants.

ABC3 Function Is Important for Host Penetration

We have shown here that *ABC3* is required for *Magnaporthe* pathogenesis and that its function is most likely critical at the host penetration step during blast disease establishment. The vast majority (~99%) of *abc3Δ* appressoria failed to breach the host surface even upon extended incubation. As judged by papillary callose deposits and TEM analyses, only a negligible number of mutant appressoria managed to make futile attempts at host penetration but were able to elicit weak HR within the host tissue during compatible and incompatible interactions as well as upon host inoculation through wounds or by injection. We feel that the

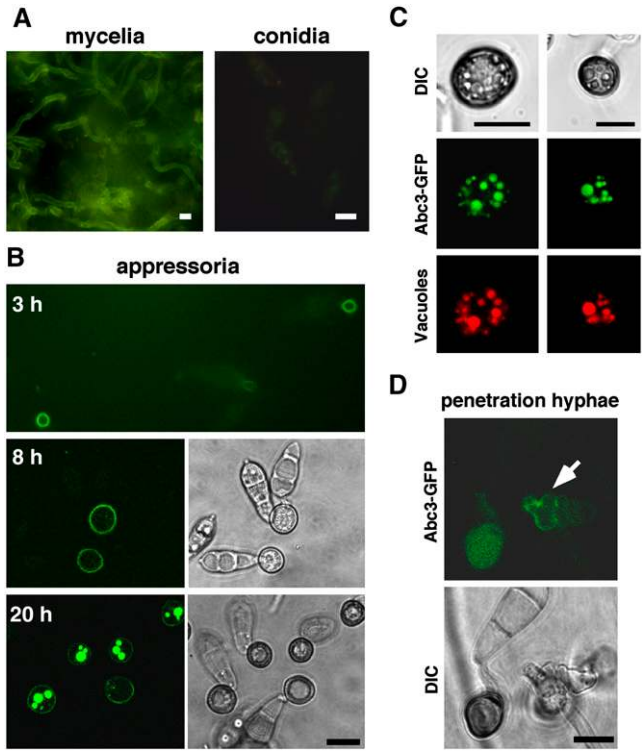

Figure 12. Subcellular Distribution of Abc3-GFP Fusion Protein.

(A) Mycelia and conidia harvested from the strain expressing an ABC3-GFP fusion protein were imaged using laser scanning confocal microscopy to detect the enhanced GFP signal. Bars = 10 μM.

(B) Appressorium development in the germ tubes of the ABC3-GFP strain was monitored over a 24-h period. At the indicated time points after germination, GFP epifluorescence was imaged to locate the Abc3-GFP fusion protein. Bar = 10 mm.

(C) Vacuolar distribution of Abc3-GFP. Appressoria formed by the Abc3-GFP strain were stained with LysoTracker Red DND-99 (left panel, vacuoles) or with Neutral Red (right panels) at the 20-h time point to visualize vacuoles. DIC, differential interference contrast. Bars = 10 μm.

(D) Confocal microscopy–assisted analysis of Abc3-GFP localization in the penetration structures (arrow) elaborated by the appressoria in PUDO-193 membrane. Bar = 10 μm.

abc3Δ-host interface still needs to be defined further in this regard and will certainly gain from recent studies that used lesion mimic mutants (Park et al., 2004) or resistant cultivars (Gilbert et al., 2006) to assess the interaction of rice with *Magnaporthe* mutants that are compromised for host penetration.

Cytorrhysis assays (Howard et al., 1991; de Jong et al., 1997) revealed that there was no significant reduction in the overall turgor generated by the *abc3Δ* appressoria, despite their average size being slightly larger than the wild-type appressoria. Interestingly, the *abc3Δ* appressoria were capable of penetrating cellophane membranes, albeit less efficiently than the wild-type strain. However, subsequent invasive growth and spread within the cellophane membranes were significantly compromised in the *abc3Δ* mutant, which also showed reduced viability under these conditions.

Accumulation of Inhibitory Metabolite(s) in the *abc3Δ* Mutant

Our results indicated that the Abc3 transporter activity is most probably required for the timely efflux of certain inhibitory metabolite(s) during the host penetration step of blast infections. Intracellular extracts from *abc3Δ* appressoria, when applied exogenously, caused a striking reduction in the wild-type strain's ability to penetrate host surfaces and cellophane membranes, thus suggesting that the *abc3Δ* mutant is defective in the efflux of toxic metabolite(s) whose accumulation in appressoria likely inhibits penetration.

The ability of *abc3Δ* to penetrate cellophane (although inefficient) is still puzzling given that the inhibitory metabolites discussed above were made from mutant appressoria on GelBond polyester films. We speculate that it is probably the amount of the inhibitory metabolite(s) and/or the timing of their production that are the limiting factors that allow the mutant to escape the maximal activity of these inhibitors on cellophane. Another likely possibility is that maximum turgor generation is probably not necessary on such surfaces. It remains to be seen whether the host surface also plays a role in the extrusion and/or the efficacy of these inhibitory metabolite(s). In preliminary experiments, exogenous addition of the toxic metabolite(s) during wild-type infection assays caused a discernable reduction in blast symptoms and elicited noticeable HR in the host leaf even in the absence of the blast fungus. Further experiments are certainly necessary to really ascertain the true nature of these HR-like symptoms. Future experiments will be directed at identifying the biochemical nature and function of these inhibitory metabolites trapped in the *abc3Δ* appressoria.

Novel Functions for Abc3-Mediated Efflux in *Magnaporthe*

Abc3 protein showed extensive similarity to several MDR-like proteins from filamentous fungi, most notably *Phaeosphaeria*, *Fusarium*, *Neurospora*, and *Aspergillus* species. Intragenome BLAST (*Magnaporthe* Genome Database, Broad Institute) searches using Abc3p as query revealed that the *Magnaporthe* genome encodes at least 76 ABC-like transporters and further helped us identify a paralog (MG09931.4; 56% similarity) within the *Magnaporthe* proteome. Such paralogs were also uncovered in *Aspergillus*, *Fusarium*, and *Neurospora* species, and their occurrence was suggestive of a recent gene duplication event. Phylogenetic analyses revealed that Abc3p most likely defines a distinct class of MDR transporters that is separate from the ones represented by Pmd1 and AtrC. Abc3p belongs to the MDR P-glycoprotein subfamily of ABC transporters that modulate the efflux of a broad range of compounds, such as sugars, inorganic ions, heavy metal ions, peptides, lipids, metabolic poisons, and drugs (Kolaczkowski et al., 1998), and effectively reduce the cellular accumulation of the target compounds by efflux from the inner leaflet of the plasma membrane to the cell exterior (Driessen et al., 2000). Abc3p could functionally replace Pmd1 (its potential ortholog from the fission yeast), and Abc3p-like Pmd1 regulated the resistance toward cyclic peptide antibiotics such as Valinomycin. It is noteworthy that the closely related AfuMDR1 (Tobin et al., 1997) from *A. fumigatus* has been shown to be specific for the antifungal agent Cilofungin, whereas AtrD, which is 76% identical to AfuMDR1, serves as an efflux pump for fenarimol (Andrade et al., 2000b). Thus, a higher degree of primary sequence homology has no bearing on similar substrate specificity. It will be interesting to see if the major efflux target of Abc3 is a novel molecule or a cyclic peptide that resembles Valinomycin.

However, a distinctive function for Abc3p, compared with its orthologs, seems to be in the regulation of oxidative stress as exemplified by our observations that loss of Abc3p renders the blast fungus highly sensitive to oxidative damage. Additionally, we confirmed that compared with the wild type, the *abc3Δ* appressoria accumulate significantly higher levels of reactive oxygen intermediates. This peroxide accretion occurred under in vitro and in planta conditions. Suppressing this peroxide accumulation through the use of antioxidants partially suppressed the host penetration defects in the *abc3Δ* mutant. Conversely, addition of exogenous peroxide, menadione, or paraquat during infection assays significantly blocked the growth and function of wild-type *Magnaporthe* conidia and appressoria. Based on the above findings, we attributed the failure of *abc3Δ* appressoria to invade the host to the cumulative effect of the following two anomalies therein: (1) accumulation of inhibitory metabolite(s) and (2) excessive buildup of reactive oxygen intermediates. It is presently unclear whether the processes leading to peroxide buildup in *abc3Δ* follow those observed in yeast and fungal mutants (Nomura and Takagi, 2004; Chen and Dickman, 2005) that frequently accumulate ROS and are also defective in mechanisms involved in resistance to oxidative stress. We could not recover viable cultures of the *abc3Δ* mutant (beyond 30 h after inoculation) from the inoculation sites in the host, allowing us to further speculate that Abc3p is likely important for in planta survival and spread of *Magnaporthe*. In preliminary analyses (data not shown), the loss of viability of the *abc3Δ* mutant appeared independent of the autophagic cell death pathway that has recently been implicated in conidial cell death during initiation of blast disease (Veneault-Fourrey et al., 2006). However, it is quite possible that the increased cell death in the mutant is a consequence of excessive ROS accumulation.

Redox Regulation and Subcellular Distribution of Abc3

An interesting finding was the redox-responsive regulation of *ABC3* expression, as judged by an *ABC3* promoter–driven destabilized

GFP reporter construct. The *ABC3* transcript was also found to be upregulated at the early stages of plant infection. It is presently unclear whether host signals directly influence *ABC3* expression during the pathogenesis cycle. Subcellular localization studies established that the Abc3-GFP fusion protein is enriched in the plasma membrane in the mycelia and the appressoria. However, a significant distribution of Abc3-GFP was also observed in the vacuoles during the late stages of appressorium maturation. Subsequently, Abc3-GFP became plasma membrane associated in the primary penetration hyphae. It remains to be seen whether this aspect of Abc3p distribution is necessary for its function and/or is required to control the effective cellular levels of Abc3p within the appressorium and/or the penetration structures.

In summary, *Magnaporthe* Abc3p is a novel MDR transporter that plays an important role during host penetration and is also involved in regulating the fungal response to intracellular oxidative stress. Future studies will focus on the identification of the specific substrate(s) effluxed by Abc3p during *Magnaporthe* pathogenesis. It will be important to find out whether Abc3 shares some function(s) with other fungal transporters (Urban et al., 1999; Vermeulen et al., 2001; Fleissner et al., 2002; Stergiopoulos et al., 2003; de Waard et al., 2006) implicated in the efflux of antimicrobial compounds within the host. Likewise, it will be interesting to assess whether the *ABC3* orthologs that we identified in several plant pathogenic fungi serve the same function in fungal virulence as their rice blast counterpart. Lastly, given that Abc3p is important for pathogenicity, resides at the plasma membrane, and is also part of the cytoplasm-to-vacuole trafficking route, we feel that it would serve as an excellent target for the intervention of the rice blast disease.

METHODS

Fungal Strains and Growth Conditions

Wild-type strains Guy11 (*mat1-2*) and TH3 (*mat1-1*) were a kind gift from Didier Tharreau (CIRAD, France), and B157 (field isolate, *mat1-2*) was obtained from the Directorate of Rice Research (Hyderabad, India). Guy11, *abc3Δ* knockout, and complementation strains were cultured on prune-agar medium or CM as described (Soundararajan et al., 2004). The mycelia, collected from 2-d-old liquid CM-grown cultures, were used for the isolation of nucleic acids. Normally, the *Magnaporthe grisea* strains were cultured for a week on solid CM media to assess the growth and colony characteristics. Mycelia used for total protein extraction were obtained by growing the relevant strains in liquid CM for 3 d at 28°C. Mating analyses were performed as described (Valent et al., 1991).

Appressorial Assays and Pathogenicity Tests

Conidia were obtained by scraping 8-d-old cultures grown under constant illumination. Mycelial bits were separated from conidia by filtration through two layers of Miracloth (Calbiochem) and resuspended to a concentration of 10^5 spores per milliliter in sterile distilled water. For light microscopy, individual droplets (30 μL) of conidial suspensions were applied to surface-sterilized plastic cover slips or other membranes and incubated under humid conditions at room temperature, and microscopic observations were made after 3, 6, 12, 24, and 36 h.

For host penetration assays, conidial suspensions in deionized water were inoculated on barley (*Hordeum vulgare* cv *Express*) leaf explants, rice (*Oryza sativa*) leaf sheaths, or onion (*Allium cepa*) epidermal strips and assessed after 24, 48, 72, or 96 h (Chida and Sisler, 1987). In these assays, fungal structures were stained by acid fuchsin as described (Balhadère et al., 1999) or by aniline blue to stain papillary callose deposit and infection hyphae (Vogel and Somerville, 2000; Jacobs et al., 2003). Penetration/infection hyphae were also detected by autofluorescence under UV light or by aniline blue staining (Jacobs et al., 2003). Pathogenicity assays using spray inoculations were performed following established protocols (Naqvi et al., 1995; Soundararajan et al., 2004). Rice seedlings of cultivar CO39 (blast susceptible) or NIL127 (blast resistant, *Pi-9*), barley seedlings, or onion epidermal strips were used for these assays. Leaf material and epidermal strips were surface sterilized prior to use in the spot inoculation assays with conidial suspensions.

Nucleic Acid and Protein-Related Manipulation

Standard molecular manipulations were performed as previously described (Sambrook et al., 1989). Fungal genomic DNA was extracted with the potassium acetate method (Naqvi et al., 1995). Plasmid DNA was isolated using the Qiagen plasmid preparation kits and nucleotide sequencing performed using the ABI Prism big dye terminator method (PE-Applied Biosystems). Homology searches of DNA/protein sequences were performed using the BLAST program (Altschul et al., 1997). GeneWise-based predictions were made using the public domain database of the European Bioinformatics Institute (http://www.ebi.ac.uk/Wise2/index.html). Total RNA was isolated with the RNeasy plant mini kit (Qiagen), and cDNA synthesis and subsequent PCR amplification were conducted using reverse transcriptase, AMV (Roche Diagnostics), and Taq DNA Polymerase (Roche). For the 5′ RACE, terminal deoxynucleotidyl transferase (Promega Biosciences) was used. The following primers were used for 5′ and 3′ RACE: Abc-5′RACE (5′-CGGAACCAGATATGAGGAGCTGTTGA-3′) and RACE-OligodT-anchor (5′-GACCACGCGTATCGATGTCGACTTTTTTTTTTTTTTTC-3′); and RACE-anchor (5′-GACCACGCGTATCGATGTCGAC-3′) and Abc-3′RACE (5′-TGATGCTGGTGTTGTACATG-3′). For semiquantitative RT-PCR experiments, the following primers were used: MgChap1F (5′-CAAGCCGATAGACACACTGAC-3′) and MGChap1R (5′-GAACTAATCGTCCTCAGTGC-3′), this ORF is not annotated but maps to contigs 2.1212 and 2.1211; MgTubF (5′-AAACAACTGGGCCAAGGGTCACTACA-3′) and MgTubR (5′-CCGATGAAAGTCGACGACATCTTGAG-3′), corresponding to ORF MG00604.4; and Abc3F (5′-CGTTATGCAGTCCATGTGGATGAGTC-3′) and Abc3R (5′-ACGATTTGTTCGCTGCGCACGTCGAT-3′). The oligonucleotide primers for the RT-PCR experiments on host were as follows: HvPr5F (5′-CGCAGAGCAACAACAGTAAAGC-3′) and HVPr5R (5′-ACGCCTATTATTGGTTGGCG-3′); and Hvact10F (5′-CTGTCTTTCCCAGCATTGTA-3′) and Hvact10R (5′-ATCCTCGGTGCGACACGGAG-3′).

For real-time RT-PCR, total RNA was extracted from the requisite samples as described (Ramos-Pamplona and Naqvi, 2006) and treated with RNAase-free DNase (Roche Diagnostics), and 1 μg was reverse-transcribed for 60 min at 42°C using the reverse transcription kit (Roche Diagnostics) in the presence of random primers and oligo(dT_{18}). Quantitative PCR was performed by monitoring in real time the increase in fluorescence of the SYBR Green dye on the real-time PCR 7900HT according to the manufacturer's instructions (Applied Biosystems). Primers used for the amplifications were Pr-1F (5′-ATGGAGGTATCCAAGCTGGCCATT-3′), Pr-1R (5′-GTAAGGCCTCTGTCCGACGAAGTT-3′), ActinF (5′-TAGTATTGTTGGCCGTCCTCGCCACAC-3′), ActinR (5′-GATGGAATGATGAAGCGCATATCCTTC-3′), HvPr5F (5′-CGCAGAGCAACAACAGTAAAGC-3′), HvPr5R (5′-ACGCCTATTATTGGTTGGCG-3′), Hvact10F (5′-CTGTCTTTCCCAGCATTGTA-3′), and Hvact10R (5′-ATCCTCGGTGCGACACGGAG-3′). Each RT-PCR quantification was performed in triplicate. Melting curve analysis was applied to all final PCR products after the cycling protocols. Values for each gene were normalized to the expression level of the respective control condition and used further to calculate the ratio of the expression levels of the requisite transcripts (for instance, *Pr-1*/*Actin*).

Protein purification and immunoblotting procedures were performed as detailed previously (Soundararajan et al., 2004). Protein concentrations were determined according to Bradford (1976) using a commercial kit (Bio-Rad Laboratories). The enhanced chemiluminescent method (ECL kit; Amersham Biosciences) was used for DNA gel blot and protein gel blot analyses.

Phylogenetic Analysis

Multiple sequence alignments were initially performed using ClustalW (Thompson et al., 1994) for the following MDR sequences related to Abc3 protein: *Mus* (ABCB1; NP_035206), *Rattus* (ABCB1a; NP_596892), *Cricetulus* (ABCB1; P21448), *Homo* (ABCB1; AAW82430), *Canis* (MDR1; AAY67840), *Ovis* (MDR1; NP_001009790), *Xenopus* (MDR11; NP_989254), *Gallus* (LOC420606; XP_418707), *Oryza* (XP_467259), *Chaetomium* (CHGG_08744; EAQ84730), *Neurospora* (reannotated NCU06011.2 and NCU9975.1), *Magnaporthe* (ABC3; AAZ81480 and MG09931.4), *Fusarium* (FG06881.1; FG03323.1; FG08823.1; FG02786.1; FG01684.1), *Aspergillus* (AAD43626; Afu7g00480; AN9342.2; AN2349.2; XP_747768; BAE64667; BAE61398; AAD25925; AAB88658; AN3608.2; XP_751944), *Coccidioides* (EAS34680; EAS30718; EAS35426), *Saccharomyces* (STE6; CAA82054); *Schizosaccharomyces* (MAM1, P78966; PMD1, CAA20363); *Ustilago* (UM06009.1), *Cryptococcus* (CNA07730), *Filobasidiella* (MDR1; AAC49890), *Yarrowia* (YALIOB12188g), *Leptosphaeria* (AAS92552), *Venturia* (AAL57243), *Trichophyton* (AAG01549), and *Phaeosphaeria* (EAT87032). Phylip 3.6a (Felsenstein, 1989) was subsequently used after removing the gaps from the initial alignment (see Supplemental Figure 1 online) to create a phylogram representing the most parsimonious phylogenetic relatedness of *Magnaporthe* Abc3p with the other MDR sequences from the indicated genera within the eukaryotes. Bootstrap analysis (500 replicates/iterations) was used to generate the phylogenetic tree using the neighbor-joining algorithm in Phylip 3.6a. Percentage bootstrap support values exceeding 50% were considered significant. The MDR hits related to Abc3p were initially identified using the B-Link web tool on the NCBI network.

Isolation of the *ABC3* Insertion Mutant

Agrobacterium tumefaciens T-DNA transfer was performed in *Magnaporthe* using hygromycin resistance (encoded by the hygromycin phosphotransferase gene *HPH1*) as a selectable marker. Copy number of the integron was identified by DNA gel blots using standard procedures (Sambrook et al., 1989). Mutant strains of interest were collected and purified by backcross analysis, progeny testing, random ascospore analysis, and by monoconidial isolation as described (Soundararajan et al., 2004). TMT2807 was obtained in the above screen as a single-copy insertional mutant that produced slightly larger appressoria and showed total loss of pathogenicity toward barley explants. DNA sequences flanking the right and left borders of the T-DNA insertion in TMT2807 were amplified using the standard thermal asymmetric interlaced PCR method (Liu et al., 1995) and subsequently confirmed by nucleotide sequencing. A mutant strain carrying the same disruption of *ABC3* as confirmed in TMT2807 was created in a Guy11 background and characterized in parallel.

ABC3 Gene Deletion and Rescue of the *abc3Δ* Mutant

DNA fragments (~1.1 kb each) representing the 5′ and 3′ untranslated regions of the *ABC3* gene were obtained by PCR, ligated sequentially so as to flank the *HPH1* cassette in pFGL44 to obtain plasmid vector pFGLabcKO. Linearized pFGLabcKO was introduced into wild-type *Magnaporthe* for a one-step replacement of the *ABC3* gene with *HPH1* cassette. The complete *Magnaporthe ABC3* locus was obtained as a 6.3-kb *Hin*dIII fragment from the BAC 22C21 and cloned into the *Hin*dIII site of pFGL97 to obtain pFGLr2 with resistance to bialaphos or ammonium gluphosinate (Cluzeau Labo) as a fungal selectable marker for the rescue transformation. DNA gel blots analyses were performed to confirm successful gene deletion strains and single-copy genomic integration of the *ABC3* rescuing cassette.

Yeast Strain, Gene Deletion, and Complementation

Schizosaccharomyces pombe wild-type strain YNB38 (*h-, ade6-M216/leu1-32/ura4-D18/his3-D1*) was obtained from David Balasundaram (Institute of Molecular Agrobiology, Singapore). It was maintained on yeast extract plus supplements (YES) agar medium or under selection on Edinburgh minimal media with appropriate supplements using standard techniques (Moreno et al., 1991). Strains were grown on agar plates or in liquid media at 32°C. One-step PCR-based gene deletion using the *Ura4+* marker was performed according to Bahler et al. (1998) using 80-bp flanking sequence homology. Deletion of the *pmd1* ORF was performed in YNB38 strain. Stable transformants from Edinburgh minimal media minus uracil medium were tested by colony PCR. The *Magnaporthe ABC3* locus was obtained as a 6.3-kb *Hin*dIII fragment from BAC 22C21 and cloned into the unique *Hin*dIII site in pJK148 to obtain pFGLr1 carrying the *Leu1+* marker. Vector pFGLr1 was linearized with *Eco*RI and transformed by electroporation into the *S. pombe pmd1* deletion strain described above. Stable integration of FGLr1 was confirmed by PCR analysis and copy number ascertained by DNA gel blot analysis.

Drug Sensitivity Tests for *Magnaporthe* and *S. pombe*

Drug sensitivity of cells was assayed by measuring the minimum inhibitory concentration. The compounds used in the drug sensitivity assays were as follows: valinomycin, verapamil, benomyl, gramicidin D, brefeldin A, leptomycin B, actinomycin D, fluconazole, and itraconazole. The cells were cultured on agar medium plates containing the specified concentration (Table 2) of each drug at 28°C for 2 to 8 d. For tests on the conidial function during pathogenic phase, the specified amounts of the compounds in the appropriate solvent were added directly to the aqueous suspension of conidia.

Extraction of Intracellular Neutral Toxins

Approximately 2×10^6 conidia (the wild type or *abc3Δ*) were inoculated in deionized water on the hydrophobic side of the GelBond membranes (BioWhittaker Molecular Applications) and allowed to form appressoria for 20 h at room temperature under high humidity. The deionized water was aspirated and the resultant appressoria washed once with chilled water, scraped immediately, and ground into a fine powder using liquid nitrogen. The homogenate was extracted with 1 mL of chloroform/methanol (1/1; v/v), and the mixture was then shaken for 10 min and centrifuged at 3000 rpm for 5 min. The extraction was then evaporated to dryness using rotary evaporation. The residue was partitioned between 1 mL *n*-hexane and 1 mL 90% methanol (1/1; v/v); the *n*-hexane layer was discarded and the methanol layer evaporated to dryness as above. The solids were then partitioned between 1 mL chloroform and 1 mL deionized water. The chloroform layer was extracted with saturated sodium hydrogen carbonate solution (3×1 mL). The chloroform layer was then concentrated to dryness and contained the neutral extraction (toxins). This was finally resuspended in 100 μL of deionized water. A parallel step involved the same procedure but without any conidia. This served as a solvent-only control for future experiments with the neutral toxins.

To obtain the extracellular toxin(s), ~2×10^6 conidia (the wild type or *abc3Δ*) were inoculated in deionized water on the hydrophobic side of the GelBond film and allowed to form appressoria for 20 h at room temperature under high humidity. All extracellular solution was collected and centrifuged to pellet the debris, and the remaining supernatant was transferred to fresh tubes and concentrated by drying in an Eppendorf

Concentrator 5301. The dried pellet was finally resuspended in 0.1 mL deionized water.

Abc3-GFP Fusion and Epifluorescence Microscopy

A 1-kb *ABC3* fragment just proximal to the translation stop codon and a 1-kb *ABC3* fragment immediately downstream of the stop were ligated into pFGL44 to flank *HPH1* marker to obtain pFGLg1. The enhanced GFP coding sequence together with the TrpC terminator was excised out of pFGL265 by *Nco*I and *Pst*I double digestion and ligated in pFGLg1 such that it was in frame with the proximal *ABC3* fragment to obtain pFGLg2. The fusion construct pFGLg2 was introduced into wild-type *Magnaporthe* using routine transformation protocols as reported earlier (Soundararajan et al., 2004). Transformants were selected on hygromycin, and the correct gene replacement event (homology-dependent chromosomal tagging of Abc3 with GFP) was confirmed by DNA gel blot and protein gel blot analyses (data not shown). The *ABC3:GFP* strains thus obtained were further tested for growth, valinomycin sensitivity, and host penetration defects to ascertain that Abc3-GFP is not compromised for function.

In a separate experiment, a 1.8-kb fragment before the translational start site of *ABC3* was used as a promoter for expressing the destabilized GFP reporter. GFP epifluorescence was observed using a Zeiss LSM510 inverted confocal microscope (Carl Zeiss) equipped with a 30-mW argon laser. The objectives were either ×63 Plan-Apochromat (numerical aperture 1.4) or a ×100 Achromat (numerical aperture 1.25) oil immersion lens. Enhanced GFP was imaged with 488-nm wavelength laser excitation, using a 505- to 530-nm band-pass emission filter, while red fluorescence was detected with a 543-nm laser and a 560-nm long-pass emission filter. Routine photomicrographs were taken using the Photometrics CoolSNAP-HQ camera mounted on a Nikon Eclipse 80i compound microscope equipped with differential interference contrast optics and the standard filters for epifluorescence detection.

Staining Methods, Drug Treatments, and Biochemical Analyses

For vacuolar staining, LysoTracker Red DND-99 (50 nM final concentration) and Neutral Red (50 nM) were used as per the manufacturer's recommendation (Invitrogen). Nitroblue tetrazolium (Sigma-Aldrich) was used at 4 mg/mL (in deionized water) and the staining performed for 1 h at room temperature prior to observation. Cell viability was measured by staining dead cells as follows: samples were stained with 20 μg/mL phloxine B (Sigma-Aldrich) for 1 h at room temperature and the samples subjected to a short wash with PBS prior to microscopic analysis and quantification. As controls for dead cells, wild-type cells were incubated for 30 min at 65°C and stained with phloxine B in parallel.

ROS were detected by staining with a solution of DAB (2 mg/mL) for 2 h followed by clearing in a solution of acetic acid:glycerol:ethanol (1:2:2) at 80°C for 5 min and subsequently stored in 3% glycerol or by staining with 2',7'-dichlorofluorescein diacetate (10 μM; in 30 mM KCl and 10 mM MES-KOH, pH 6) for 1 h at room temperature. For fungus-inoculated leaf material, the DAB and Trypan blue stainings were essentially as described (Thordal-Christensen et al., 1997; Gilbert et al., 2006, respectively). In the costaining method, DAB was used prior to sample clarification and Trypan blue treatment. Antioxidants ascorbic acid and *N*-acetylcysteine were used at 5 mM concentration and were purchased from Sigma-Aldrich.

The intracellular formation of ROS in appressoria was quantified using the fluorescent probe CM-DCFDA (Invitrogen). The appressorial preparation from the requisite strain was washed two times in PBS and exposed to 50 μM CM-DCFDA in PBS for 1 h at 28°C. The appressoria then were washed two times in PBS, solubilized in water, and homogenized in a Mini Bead beater to obtain the intracellular extracts. The fluorescence was determined at 488/525 nm, normalized on a protein basis, and expressed as fold change over the wild-type control, which was arbitrarily set at 1.

For preparing barley leaf extracts, fresh samples from 21-d-old seedlings were surface sterilized and ground to a fine powder using liquid nitrogen in a mortar and stirred in cold, sterilized distilled water. Ten milliliters of water per gram of leaf material was added to the sample. The mixture was kept in a refrigerator for 2 h and then stirred on a rotary shaker for 1 h and centrifuged at 5000 rpm for 15 min. The supernatant was collected and stored in a refrigerator until it was used as a crude water-soluble extract.

Accession Numbers

Sequence data from this article can be found in the GenBank/EMBL data libraries under accession numbers DQ156556 (*ABC3*), U89895 (*Pr-1*), AC104285 (*Actin*), AJ276225 (*HvPr5*), and U21907 (*Hvact10*).

Supplemental Data

The following materials are available in the online version of this article.

Supplemental Figure 1. Multiple Sequence Alignment Used for the Phylogenetic Analysis of Abc3-Related MDR Proteins.

Supplemental Figure 2. Phylogram of Multidrug Resistance Proteins Related to *Magnaporthe* Abc2p.

Supplemental Figure 3. Clustal Alignment of *Magnaporthe* Transporters Abc1 and Abc3.

ACKNOWLEDGMENTS

We thank Patricia Netto for the excellent TEM support. We also thank Liu Yuan Yuan and Shanthi Soundararajan for the invaluable help during mutant screenings and members of the Fungal Patho-Biology Group, in particular Marilou Ramos-Pamplona and Rajesh Patkar, for discussions and suggestions. We thank Marc-Henri Lebrun for providing the PUDO-193 membrane and Alan Christoffels, Gen Hua, and Julian Lai for help with the phylogenetic analyses. This work was supported by intramural research funds from the Temasek Life Sciences Laboratory of Singapore.

Received September 12, 2005; revised September 22, 2006; accepted November 10, 2006; published December 22, 2006.

REFERENCES

Altschul, S.F., Madden, T.L., Shaffer, A.A., Zhang, Z., Miller, W., and Lipman, D.J. (1997). Gapped BLAST and PSI-BLAST: A new generation of protein database search programs. Nucleic Acids Res. **25,** 3389–3402.

Andrade, A.C., Del Sorbo, G., van Nistelrooy, J.G.M., and De Waard, M.A. (2000). The ABC transporter AtrB from *Aspergillus nidulans* mediates resistance to all major classes of fungicides and some natural toxic compounds. Microbiology **146,** 1987–1997.

Andrade, A.C., van Nistelrooy, J.G.M., Peery, R.B., Skatrud, P.L., and De Waard, M.A. (2000b). The role of ABC transporters from *Aspergillus nidulans* in protection against cytotoxic agents and in antibiotic production. Mol. Gen. Genet. **263,** 966–977.

Bahler, J., Wu, J.Q., Longtine, M.S., Shah, N.G., McKenzie, A., 3rd, Steever, A.B., Wach, A., Philippsen, P., and Pringle, J.R. (1998). Heterologous modules for efficient and versatile PCR-based gene targeting in *Schizosaccharomyces pombe.* Yeast **14,** 943–951.

Balhadère, P., Foster, A., and Talbot, N.J. (1999). Identification of pathogenicity mutants of the rice blast fungus *Magnaporthe grisea* by insertional mutagenesis. Mol. Plant Microbe Interact. **12,** 129–142.

Bradford, M.M. (1976). A rapid and sensitive method for the quantitation of microgram quantities of protein utilizing the principle of protein-dye binding. Anal. Biochem. **72,** 248–254.

Chen, C., and Dickman, M.B. (2005). Proline suppresses apoptosis in the fungal pathogen *Colletotrichum trifolii.* Proc. Natl. Acad. Sci. USA **102,** 3459–3464.

Chiarugi, P., Pani, G., Giannoni, E., Taddei, L., Colavitti, R., Raugei, G., Symons, M., Borrello, S., Galeotti, T., and Ramponi, G. (2003). Reactive oxygen species as essential mediators of cell adhesion: The oxidative inhibition of a FAK tyrosine phosphatase is required for cell adhesion. J. Cell Biol. **161,** 933–944.

Chida, T., and Sisler, H.D. (1987). Restoration of appressorial penetration ability by melanin precursors in *Pyricularia oryzae* treated with anti-penetrants and in melanin-deficient mutants. J. Pestic. Sci. **12,** 49–55.

Clergeot, P.H., Gourgues, M., Cots, J., Laurans, F., Latorse, M.P., Pepin, R., Tharreau, D., Notteghem, J.L., and Lebrun, M.H. (2001). *PLS1*, a gene encoding a tetraspanin-like protein, is required for penetration of rice leaf by the fungal pathogen *Magnaporthe grisea.* Proc. Natl. Acad. Sci. USA **98,** 6963–6968.

Cole, S.P., Bhardwaj, G., Gerlach, J.H., Mackie, J.E., Grant, C.E., Almquist, K.C., Stewart, A.J., Kurz, E.U., Duncan, A.M., and Deeley, R.G. (1992). Overexpression of a transporter gene in a multidrug-resistant human lung cancer cell line. Science **258,** 1650–1654.

Daniele, R.P., and Holian, S.K. (1976). A potassium ionophore (valinomycin) inhibits lymphocyte proliferation by its effects on the cell membrane. Proc. Natl. Acad. Sci. USA **73,** 3599–3602.

Decottignies, A., and Goffeau, A. (1997). Complete inventory of the yeast ABC proteins. Nat. Genet. **15,** 137–145.

de Jong, J.C., McCormack, B.J., Smirnoff, N., and Talbot, N.J. (1997). Glycerol generates turgor in rice blast. Nature **389,** 244–245.

de Waard, M.A., Andrade, A.C., Hayashi, K., Schoonbeek, H.J., Stergiopoulos, I., and Zwiers, L.H. (2006). Impact of fungal drug transporters on fungicide sensitivity, multidrug resistance and virulence. Pest Manag. Sci. **62,** 195–207.

Dixon, R.A., Harrison, M.J., and Lamb, C.J. (1994). Early events in the activation of plant defense responses. Annu. Rev. Phytopathol. **32,** 479–501.

Driessen, A.J.M., Rosen, B.P., and Konings, W.N. (2000). Diversity of transport mechanisms: common structural principles. Trends Biochem. Sci. **25,** 397–401.

Felsenstein, J. (1989). PHYLIP (phylogeny inference package). Version 3.2. Cladistics **5,** 164–166.

Fleissner, A., Sopalla, C., and Weltring, K.M. (2002). An ATP-binding cassette multidrug-resistance transporter is necessary for tolerance of *Gibberella pulicaris* to phytoalexins and virulence on potato tubers. Mol. Plant Microbe Interact. **15,** 102–108.

Gilbert, M.J., Thornton, C.R., Wakley, G.E., and Talbot, N.J. (2006). A P-type ATPase required for rice blast disease and induction of host resistance. Nature **440,** 535–539.

Gottesman, M.M., and Pastan, I. (1993). Biochemistry of multidrug resistance mediated by the multidrug transporter. Annu. Rev. Biochem. **62,** 385–427.

Hamer, J.E., and Talbot, N.J. (1998). Infection-related development in the rice blast fungus *Magnaporthe grisea.* Curr. Opin. Microbiol. **1,** 693–697.

Higgins, C.F. (1992). ABC transporters: From microorganisms to man. Annu. Rev. Cell Biol. **8,** 67–113.

Howard, R.J., Ferrari, M.A., Roach, D.H., and Money, N.P. (1991). Penetration of hard substrates by a fungus employing enormous turgor pressures. Proc. Natl. Acad. Sci. USA **88,** 11281–11284.

Jacobs, A.K., Lipka, V., Burton, R.A., Panstruga, R., Strizhov, N., Schulze-Lefert, P., and Fincher, G.B. (2003). An *Arabidopsis* callose synthase, GSL5, is required for wound and papillary callose formation. Plant Cell **15,** 2503–2513.

Ketchum, C.J., Schmidt, W.K., Rajendrakumar, G.V., Michaelis, S., and Maloney, P.C. (2001). The yeast a-factor transporter Ste6p, a member of the ABC superfamily, couples ATP hydrolysis to pheromone export. J. Biol. Chem. **276,** 29007–29011.

Kimura, O., Endo, T., Hotta, Y., and Sakata, M. (2005). Effects of P-glycoprotein inhibitors on trans-epithelial transport of cadmium in cultured renal epithelial cells, LLC-PK1 and LLC-GA5–COL150. Toxicology **208,** 123–132.

Kodama, O., Miyakawa, J., Akatsuka, T., and Kiyosawa, S. (1992). Sakuranetin, a flavonone phytoalexin from ultraviolet-irradiated rice leaves. Phytochemistry **31,** 3807–3809.

Kolaczkowski, M., Kolaczowska, A., Luczynski, J., Witek, S., and Goffeau, A. (1998). In vivo characterization of the drug resistance profile of the major ABC transporters and other components of the yeast pleiotropic drug resistance network. Microb. Drug Resist. **4,** 143–158.

Kumar, S., Tamura, K., and Nei, M. (2004). MEGA 3: Integrated software for molecular evolutionary genetics analysis and sequence alignment. Brief. Bioinform. **5,** 150–163.

Lee, Y.J., Yamamoto, K., Hammamoto, H., Nakaune, R., and Hibi, T. (2005). A novel ABC transporter gene ABC2 involved in multidrug susceptibility but not pathogenicity in rice blast fungus, *Magnaporthe grisea.* Pestic. Biochem. Physiol. **81,** 13–23.

Lev, S., Hadar, R., Amedeo, P., Baker, S.E., Yoder, O.C., and Horwitz, B. (2005). Activation of an AP1-like transcription factor of the maize pathogen *Cochliobolus heterostrophus* in response to oxidative stress and plant signal. Eukaryot. Cell **4,** 443–454.

Liu, Y.G., Mitsukawa, N., Oosumi, T., and Whittier, R.F. (1995). Efficient isolation and mapping of *Arabidopsis thaliana* T-DNA insert junctions by thermal asymmetric interlaced PCR. Plant J. **8,** 457–463.

Michaelis, S., and Berkower, C. (1995). Sequence comparison of yeast ATP-binding cassette proteins. Cold Spring Harb. Symp. Quant. Biol. **LX,** 291–307.

Moreno, S., Klar, A., and Nurse, P. (1991). Molecular genetic analysis of fission yeast *Schizosaccharomyces pombe.* Methods Enzymol. **194,** 795–823.

Naqvi, N.I., Bonman, J.M., Mackill, D.J., Nelson, R.J., and Chattoo, B.B. (1995). Identification of RAPD markers linked to a major gene for blast resistance in rice. Mol. Breed. **1,** 341–348.

Nishi, K., Yoshida, M., Nishimura, M., Nishikawa, M., Nishiyama, M., Horinouchi, S., and Beppu, T. (1992). A leptomycin B resistance gene of *Schizosaccharomyces pombe* encodes a protein similar to the mammalian P-glycoproteins. Mol. Microbiol. **6,** 761–769.

Nomura, M., and Takagi, H. (2004). Role of the yeast acetyltransferase Mpr1 in oxidative stress: Regulation of oxygen reactive species caused by a toxic proline catabolism intermediate. Proc. Natl. Acad. Sci. USA **101,** 12616–12621.

Osbourn, A.E. (1996). Preformed antimicrobial compounds and plant defense against fungal attack. Plant Cell **8,** 1821–1831.

Ou, S.H. (1985). Rice Diseases. (Surrey, UK: Commonwealth Mycological Institute).

Park, G., Bruno, K.S., Staiger, C.J., Talbot, N.J., and Xu, J.R. (2004). Independent genetic mechanisms mediate turgor generation and penetration peg formation during plant infection in the rice blast fungus. Mol. Microbiol. **53,** 1695–1707.

Ramos-Pamplona, M., and Naqvi, N.I. (2006). Host invasion during rice-blast disease requires carnitine-dependent transport of peroxisomal acetyl-CoA. Mol. Microbiol. **61,** 61–75.

Routledge, A.P.M., Shelly, G., Smith, J.V., Talbot, N.J., Draper, J., and Mur, L.A.J. (2004). *Magnaporthe grisea* interactions with the model grass *Brachypodium distachyon* closely resemble those with rice (*Oryza sativa*). Mol. Plant Pathol. **5,** 253–265.

Saier, M.H., Jr., and Paulsen, I.T. (2001). Phylogeny of multidrug transporters. Semin. Cell Dev. Biol. **12,** 205–213.

Sambrook, J., Fritsch, E.F., and Maniatis, T. (1989). Molecular Cloning: A Laboratory Manual. (Cold Spring Harbor, NY: Cold Spring Harbor Laboratory Press).

Soundararajan, S., Jedd, G., Li, X., Ramos-Pamplona, M., Chua, N.H., and Naqvi, N.I. (2004). Woronin body function in *Magnaporthe grisea* is essential for efficient pathogenesis and for survival during nitrogen starvation stress. Plant Cell **16,** 1564–1574.

Stergiopoulos, I., Zwiers, L.H., and De Waard, M.A. (2003). The ABC transporter MgAtr4 is a virulence factor of *Mycosphaerella graminicola* that affects colonization of substomatal cavities in wheat leaves. Mol. Plant Microbe Interact. **16,** 689–698.

Talbot, N.J. (2003). On the trail of a cereal killer: Exploring the biology of *Magnaporthe grisea.* Annu. Rev. Microbiol. **57,** 177–202.

Thompson, J.D., Higgins, D.G., and Gibson, T.J. (1994). CLUSTAL W: Improving the sensitivity of progressive multiple sequence alignment through sequence weighting, position-specific gap penalties and weight matrix choice. Nucleic Acids Res. **22,** 4673–4680.

Thordal-Christensen, H., Zhang, Z., Wei, Y., and Collinge, D.B. (1997). Subcellular localization of H_2O_2. H_2O_2 accumulation in papillae and hypersensitive response during the barley-powdery mildew interaction. Plant J. **11,** 1187–1194.

Tobin, M.B., Peery, R.B., and Skatrud, P.L. (1997). Genes encoding multiple drug resistance-like proteins in *Aspergillus fumigatus* and *Aspergillus flavus.* Gene **200,** 11–23.

Uhr, M., Holsboer, F., and Muller, M.B. (2002). Penetration of endogenous steroid hormones corticosterone, cortisol, aldosterone and progesterone into the brain is enhanced in mice deficient for both mdr1a and mdr1b P-glycoproteins. J. Neuroendocrinol. **14,** 753–759.

Urban, M., Bhargava, T., and Hamer, J.E. (1999). An ATP-driven efflux pump is a novel pathogenicity factor in rice blast disease. EMBO J. **18,** 512–521.

Valent, B. (1990). Rice blast as a model system for plant pathology. Phytopathology **80,** 33–36.

Valent, B., Farrall, L., and Chumley, F.G. (1991). *Magnaporthe grisea* genes for pathogenicity and virulence identified through a series of backcrosses. Genetics **127,** 87–101.

Veneault-Fourrey, C., Barooah, M., Egan, M., Wakley, G., and Talbot, N.J. (2006). Autophagic fungal cell death is necessary for infection by the rice blast fungus. Science **312,** 580–583.

Vermeulen, T., Schoonbeek, H., and de Waard, M.A. (2001). The ABC transporter BcatrB from *Botrytis cinerea* is a determinant of the activity of the phenylpyrrole fungicide fludioxonil. Pest Manag. Sci. **57,** 393–402.

Vogel, J., and Somerville, S. (2000). Isolation and characterization of powdery mildew-resistant *Arabidopsis* mutants. Proc. Natl. Acad. Sci. USA **97,** 1897–1902.

Zwiers, L.H., Stergiopoulos, I., Gielkens, M.M., Goodall, S.D., and de Waard, M.A. (2003). ABC transporters of the wheat pathogen *Mycosphaerella graminicola* function as protectants against biotic and xenobiotic toxic compounds. Mol. Genet. Genomics **269,** 499–507.